

# Strategic R&D Programme on Technologies for Future Experiments

*Annual Report 2020*

CERN

Experimental Physics Department

April 2021





## List of authors

### EP-R&D fellows and students

Pablo Antoszczuk, Mattia Balutto, Maria Barba Higuera, Mateus Barreto Pinto, Mateusz Karol Baszczyk, Marina Beguin, Erica Brondolin, Florian Brunbauer, Eric Buschmann, Roberto Cala<sup>1</sup>, Leonardo Cecconi, Esteban Curras Rivera, Florian Dachs, Joao De Melo, Wenjing Deng, Matheo Dias, Dominik Dobrijevic, Ana Dorda Martin, Katharina Dort, Placido Fernandez Declara, Brieuc Francois, Paul Gessinger-Befurt, Vagelis Gkougkousis, Melwin Gose, Jonas Hahnfeld, Jakob Haimberger, Marius Halvorsen, Geun Hee Hong, Desiree Hellenschmidt, Djunes Janssens, Moritz Kiehn, Adam Klekotko, Jens Kroeger, Milana Lalovic, Javier Lopez Gomez, Filip Maciej Malinowski, Demetrio Magatti, Loris Martinazzoli, Maria Molina Gonzalez, Vendula Maulerova, Magdalena Munker, Michela Neroni, Vincenzo Padulano, Risto Pejasinovic, Francesco Piro, Thorben Quast, Mateusz Karol Baszczyk, Dalila Salamani, Matteo Salomoni, Lucian Scharenberg, Shuvay Singh, Lorenzo Teofili, Gennaro Termo, Antonija Utrobicic, Tomas Vanat, Mateus Vicente, Valentin Volkl, Morag Jean Williams, Chaowaroj Wanotayaroj, Moritz Wiehe, Stefan Wunsch

### EP-R&D WP leaders + deputies

Martin Aleksa, Jakob Blomer, Michael Campbell, Victor Coco, Paula Collins, Benoit Cure, Carmelo D'Ambrosio, Dominik Dannheim, Federico Faccio, Corrado Gargiulo, Matthias Mentink, Michael Moll, Paulo Rodrigues Simoes Moreira, Eraldo Oliveri, Paolo Petagna, Christoph Rembser, Petra Riedler, Walter Snoeys, Graeme Stewart, Jan Troska

### EP-R&D steering committee members

David Barney, Roger Forty, Patrick Janot, Christian Joram, Manfred Krammer, Lucie Linssen, Christoph Rembser, Werner Riegler, Burkhard Schmidt, Andreas Schopper, Francois Vasey, Pere Mato Vila

### EP-R&D Participants

Gianluca Aglieri, Sophie Baron, Stefan Biereigel, Anthony Frederick Bulling, Jan Buytaert, Stephane Detraz, Raphael Dumps, Diego Alvarez Feito, Gabriele Fiorenza, Massimo Angeletti, Rafael Ballabriga, Jacob Bastian Van Beelen, Davide Ceresa, Andrea Catinaccio, Mara Corbetta, Roberto Guida, Pieter Ijzermans, Kostas Kloukinas, Alex Kluge, Antonio Lafuente, Elisa Laudi, Gael Ledey, Edgar Cid Lemos, Marta Lisowska, Beatrice Mandelli, Eduardo Brandao De Souza Mendes, Hans Muller, Luciano Musa, Lauri Olantera, Rui De Oliveira, Heinz Pernegger, Olivier Pizzirusso, Thenia Prousalidi, Gianluca Rigoletti, Leszek Ropelewski, Carmelo Scarcella, Heinrich Schindler, Thomas Schneider, Pascal Secouet, Csaba Soos, Miranda Van Stenis, Antonio Teixeira, Jan Troska, Rob Veenhof, Pedro Vicente Leitao

## Table of Contents

Introduction.....	7
WP1.1 Hybrid Silicon Pixel Detectors .....	9
1. Introduction.....	9
2. Main activities and achievements in 2020.....	9
2.1. Sensor development and characterisation .....	9
2.2. Hybrid sensor simulation .....	11
2.3. Fast and high-rate telescope and other timing setup.....	12
2.4. IC block design.....	13
3. Publications and contributions to conferences and workshops.....	13
4. References.....	13
WP1.2 Monolithic Silicon Pixel Detectors .....	14
1. Introduction.....	14
2. Main activities and achievements in 2020.....	14
2.1. Common technology evaluation and validation .....	14
2.2. Submissions for fabrication in 180 nm.....	15
2.3. TCAD and Monte Carlo simulation.....	16
2.4. 180 nm measurements .....	16
3. Publications and contributions to conferences and workshops.....	18
WP1.3 Silicon Modules .....	20
1. Introduction.....	20
2. Main activities and achievements in 2020.....	20
2.1. Thinning and Dicing studies .....	20
2.2. Hybridisation with fine-pitch bump bonding.....	21
2.3. Hybridisation and module integration with Anisotropic Conductive Film (ACF).....	21
2.4. Multi-chip module studies and test .....	23
3. Publications and contributions to conferences and workshops.....	24
WP1.4 Silicon Detectors – Characterization and Simulation.....	24
1. Introduction.....	24
2. Main activities and achievements in 2020 .....	25
2.1. Characterization Tools.....	25
2.2. Radiation-damage studies and damage models.....	26
2.3. Radiation damage and radiation monitoring techniques .....	28
2.4. Advanced simulation packages.....	28
2.5. Low Gain Avalanche Detectors .....	29
3. Selected publications.....	29

Contributions to conferences and workshops.....	30
WP2 Gas Detectors .....	31
1. Introduction.....	31
2. Main activities and achievements in 2020.....	31
2.1 Precise timing (25 ps): toward a large area and robust PICOSEC Micromegas .....	31
2.2 Modelling and simulation: Signal induction with resistive electrodes. ....	32
2.3 Front End Electronics: BNL/ATLAS VMM3a and RD51 SRS .....	33
2.4 Gas Studies: eco-friendly gases and fluorine based impurities. ....	34
3 Publications and contributions to conferences and workshops.....	34
WP3 Calorimetry .....	36
WP3.1 Noble Liquid Calorimetry .....	36
1. Introduction.....	36
2. Main activities and achievements in 2020.....	36
2.1 Read-out electrode design optimization.....	36
2.2 High-density signal feedthroughs .....	37
2.3 Publications and contributions to conferences and workshops.....	38
WP3.2 & WP3.2.1: R&D on SPACAL Calorimeter and Prospective R&D for Scintillator Based Calorimeters .....	38
1. Introduction.....	38
2. Main activities and achievements in 2020.....	38
2.1 R&D on garnet materials.....	38
2.2 SPACAL Calorimeter simulation .....	39
2.3 Test beam @ DESY .....	39
2.4 Publications and contributions to conferences and workshops.....	41
WP3.3: R&D for Si based calorimetry (Postponed).....	42
WP3.4: R&D on RICH detectors (activity starts in 2021).....	42
WP3.5: R&D on plastic scintillating fibre trackers .....	42
WP4 Mechanics .....	43
1. Introduction.....	43
2. Main activities and achievements in 2020.....	44
2.1. Low Mass Structure.....	44
2.2. Robotics.....	46
3. Publications and contributions to conferences and workshops.....	47
WP5 IC Technologies .....	48
1. Introduction.....	48
2. Main activities and achievements in 2020.....	48

2.1.	IC Technologies (WP 5.1).....	48
2.2.	Power distribution (WP 5.2b).....	48
3.	Publications and contributions to conferences and workshops.....	50
WP6	High Speed Links.....	51
1.	Introduction.....	51
2.	Main activities and achievements in 2020.....	51
	FPGA-1: FPGA-based system testing and emulation .....	51
	OPTO-1: Silicon Photonics System & Chip Design.....	53
	OPTO-2: Silicon Photonics Radiation Hardness .....	55
3.	Publications and contributions to conferences and workshops.....	56
WP7	Software .....	57
1.	Introduction.....	57
2.	Main activities and achievements in 2020.....	57
2.1	Turnkey Software Stack.....	57
2.2	Reconstruction – Calorimetry .....	58
2.3	Reconstruction - Tracking .....	59
2.4	Efficient Analysis .....	60
3.	Publications and contributions to conferences and workshops.....	61
WP8	Detector Magnets R&D .....	62
1.	Introduction.....	62
2.	Main activities and achievements in 2020.....	62
2.1.	4-T magnet facility.....	62
2.2.	Quench protection studies.....	64
2.3.	ATLAS Toroidal Magnet snubber.....	64
2.4.	Cryogenics .....	65
3.	Summary .....	65
4.	References.....	65

## Introduction

In autumn 2017, an initiative was launched to conceive and establish a strategic R&D program on technologies for future experiments. It was initiated by the Head of the Experimental Physics department of CERN and is also referred to as the EP R&D program.

The EP R&D program is strategic in the sense that it aims at developing those key detector technologies which will be needed for the next generation of experiments. The results of this R&D will be building blocks, demonstrators and prototypes, without already being application specific.

The landscape of particle physics at the high energy frontier is well defined until the High Luminosity upgrade of the LHC (HL-LHC) has been completed, scheduled for the long shutdown LS3 (2025-2027). With the full exploitation of the potential of the HL-LHC as clear top priority for the next 15 years, a number of studies for a major post-LHC project at CERN are being pursued: CLIC, FCC-hh, FCC-ee.

Recently, the 2020 update of the European strategy for particle physics has identified an electron-positron Higgs factory as the highest-priority next collider. For the longer term, a proton-proton collider at the highest achievable energy (at least 100 TeV) is the goal, while the  $e^+e^-$  collider could be a first stage for the machine. In addition to the accelerator R&D to prove the technical and financial feasibility of this future circular collider, the European strategy update document also clearly highlights the need to keep a strong focus on instrumentation and state-of-the-art infrastructures. Instrumentation remains a key ingredient for progress in experimental high energy physics.

Throughout the years 2018 and 2019, in a series of public meetings with strong participation of external groups, the R&D workplan emerged in a process that was largely bottom-up driven. The proposals of key technologies to be pursued and further developed exceeded the expected budget envelope and prioritisation by the Steering Committee<sup>1</sup> was unavoidable. In addition to the scientific need, also the expertise and infrastructure available at CERN played a role in the choice of topics. A further factor to be considered was the special role that CERN plays in a number of transverse technologies like ASIC design, high-speed optical links, mechanics and detector cooling, software, and experiment magnets. Some of these technologies require a critical mass which goes beyond the size of most university groups. The result was a set of 11 work packages, where the first four are focused on different aspects of Si pixel sensors (hybrid and monolithic). One work package targets new developments in gaseous detectors and another one focuses on calorimetry and light based detectors (such as RICH and scintillating fibre tracking). Five more work packages deal with the above-mentioned transverse technologies that will play crucial roles in any future experiment. The work program was documented in a comprehensive report<sup>2</sup>.

The R&D program was presented in spring 2019 to the CERN Enlarged Directorate and was approved for an initial period of five years (2020-2024). The resource situation did not allow to grant, at this stage, the budget estimated for the full program. To partially compensate for this shortcoming, an arrangement was made with the four LHC experiments and the three EP support groups. They contribute about 10% of their fellow and student quota to the R&D program. In return, every R&D fellow can spend up to six months in other (non-R&D) projects of the experiment or the support group. Parts of the proposed programme were descoped or postponed.

---

<sup>1</sup> The Steering Committee has members from all large LHC experiments, the EP support groups and representatives of the above-mentioned studies.

<sup>2</sup> Strategic R&D Programme on Technologies for Future Experiments, December 2018, CERN-OPEN-2018-006

All work packages are open to external participants and, in many cases, the cooperation relies on structures grown over many years in detector projects. In the domains of radiation hard silicon and gaseous detectors the work packages overlap on purpose with the activities of the RD50 and RD51 collaborations, leading to synergy and flexibility. Several EP R&D work packages will profit from the EU financed AIDAInnova Research Infrastructure project kicking-off in April 2021. Even if the direct financial impact is small, the cooperation and exchange with other groups will be highly beneficial for both sides.

The workplan of the R&D program foresees a major part of the work to be done by fellows and Technical or Doctoral students, while staff members spend a fraction of their time to supervise and support the fellows and students, or, as WP Leaders, steer the research work.

Recruitment of fellows and students started in autumn 2019 (committees AFC-2019-2 and TSC-2019-2) and continued in 2020. As a consequence of the covid-19 pandemic, recruitment of both fellows and students was slower than planned. Also the start-up of the individual work packages and integration of the students and fellows was more challenging than foreseen, leading in the end also to lower material expenditure than planned. The delays are typically on the level of a few months and expected to be recovered in the current and next year.

This first Annual Report presents the activities in all eleven work packages and main achievements made in 2020. The fellows and students were also encouraged to play an active role in the editing process. Given the unusual circumstances under which this R&D program had to take off, the wealth of activities and results underlines the outstanding motivation and effort of all participants.



## WP1.1 Hybrid Silicon Pixel Detectors

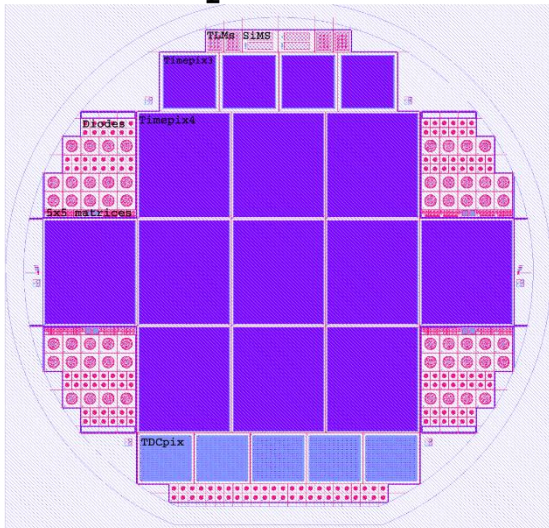
### 1. Introduction

WP 1.1 focuses on hybrid silicon sensors for charged particle detection. It targets intensity frontier applications that require specialized sensor and/or complex ASIC features: high fluence ( $>10^{16} \text{neq/cm}^2$ ), high hit rate  $O(10 \text{ Ghits/s/cm}^2)$  and/or high output bandwidth  $O(100 \text{ Gb/s})$  with spatial resolution below  $10 \mu\text{m}$  and temporal resolution below  $50 \text{ ps}$ . The work plan is articulated around four axes: the development of sensors matching the targeted resolutions under the fluences discussed above as well as their characterisation pre- and post-irradiation, the development of simulation tools allowing to understand the sensor characteristics and to aid the design process, the development of a fast timing and high rate telescope based on the Timepix4 ASIC to both characterise sensors and study system level timing, and the design of integrated electronics capable of handling the sensor signals at high rate. The WP work plan is tightly linked to the work done in the WP 1.2, 1.4 and 5, as well as with other R&D initiatives such as RD50, AIDA-innova (Timepix4 planes for EUDET telescope, iLGAD production), other institutes' R&D (collaboration with Nikhef, CPPM, USC, ...) and CERN experiment upgrades (LHCb, NA62, ...).

### 2. Main activities and achievements in 2020

The sensor development activities in 2020 were focussed on providing reference devices for the rest of the work program and exploring the limits of planar sensor technology for timing measurements. In addition, sensors with internal gain were investigated, in particular to address potential limitations arising from segmentation and radiation. Simulation tools were prepared to simulate the signal that will be generated in planar sensors of various thickness under various fluences. The design for the fast-timing telescope mechanics and cooling system was investigated.

#### ADVACAM planar sensors



#### CNM inverted LGAD

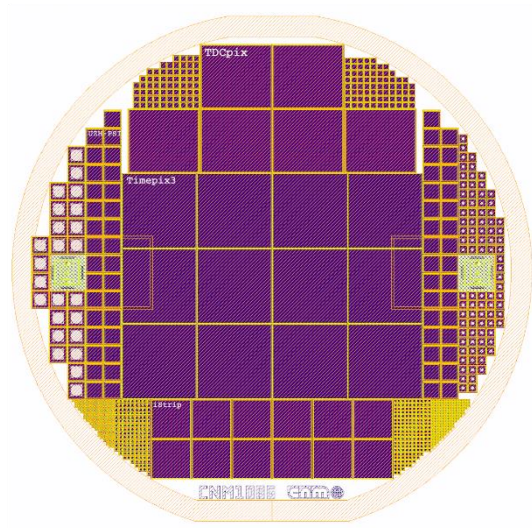


Figure 1: The layout of the wafer for planar sensor production by ADVACAM. Thicknesses of 50,100,200 and 300 $\mu\text{m}$  will be available (left); the layout of the iLGAD wafer designed by CNM in the context of a RD50 and AIDA-innova project (right).

#### 2.1. Sensor development and characterisation

A **production of n-in-p planar sensor wafers** was prepared. It features multiple wafer thickness (from  $50\mu\text{m}$  to  $300\mu\text{m}$ ), several sensor geometries matching ASICs with precise per pixel timestamp (Timepix4, TDCpix) and a set of structures for R&D. The R&D structures will allow systematic studies of the timing properties of planar technology as function of sensor thickness and integrated fluence and will provide benchmarks to test simulation tools discussed in 2.2. The large-scale sensors for TDCpix and Timepix4 sensors will allow the investigation of ASIC level timing issues. The Timepix4

sensors will in addition be used for the Timepix4 telescope discussed in 2.3. The layout of the wafer, designed by ADVACAM, is shown Figure 1 left. In parallel the WP participates, through a RD50 project, to the **production of pixelated iLGADs wafers**, also shown in Figure 1 right. It features the same full sensor footprints as the planar production. iLGAD technology increases the fill-factor of traditional LGADs by implementing the multiplication layer on the backside of the sensor, making it independent of the readout segmentation [1]. This should give the possibility of smaller pixels with greater efficiency and improved spatial resolution. The CNM production is expected for the second half of 2021.

One of the known limitations of **LGADs**, is the **degradation of gain with radiation**. A CNM production of LGADs with three gain layer dopants: Boron (B), Gallium (Ga) and Boron+Carbon (B+C); was studied after proton and neutron irradiation. The performance of the sensors was evaluated at different temperatures (-10 °C, -20 °C, -30 °C) and it was demonstrated that the active implant degrades in the same way independently of the dopant type and radiation species. This behaviour is consistent with an exponential decrease law with respect to the non-NIEL corrected fluence, as illustrated on Figure 2 left. The effective implant was subsequently probed through comparison of gain and non-gain regions. Results were corrected for deep-acceptor level re-introduction rates as defined by the RD-48 collaboration. A clear improvement is observed for B+C implants, where the post-irradiation effective doping is double the one estimated from the B only case. In contrast, Ga doped samples exhibit a 20% degradation. The effective dopant for neutron irradiation is presented on Figure 2 right. The study also demonstrated that for all implant species and all temperatures, if a signal-to-noise ratio of 18 is achieved, then an efficiency above 90% can be expected. In highly irradiated samples ( $>1e15$   $n_{eq}/cm^2$ ) where signal-to-noise ratios lower than 18 are observed, greater than 90% efficiency is still possible if bias voltage allows for a gain of 4 ( $>2$  fQ collected charge).

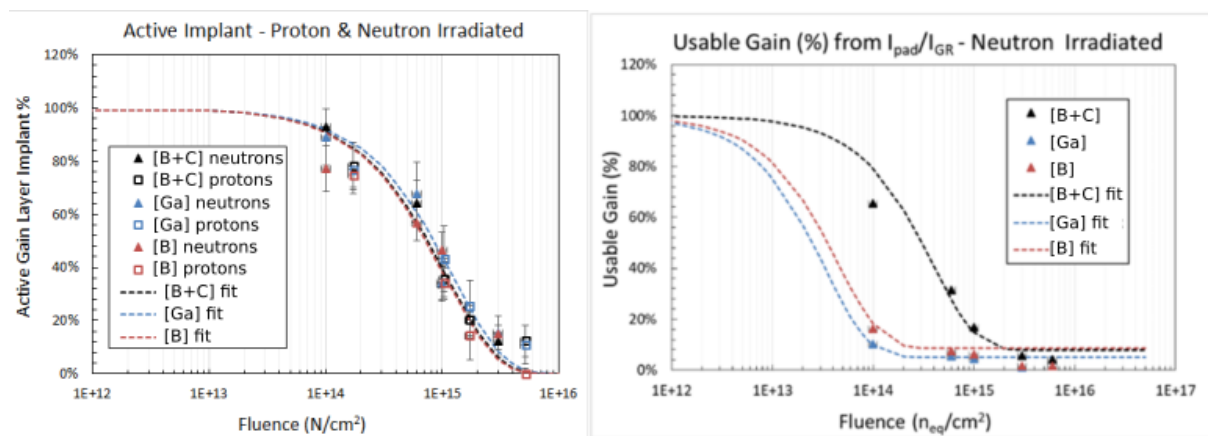
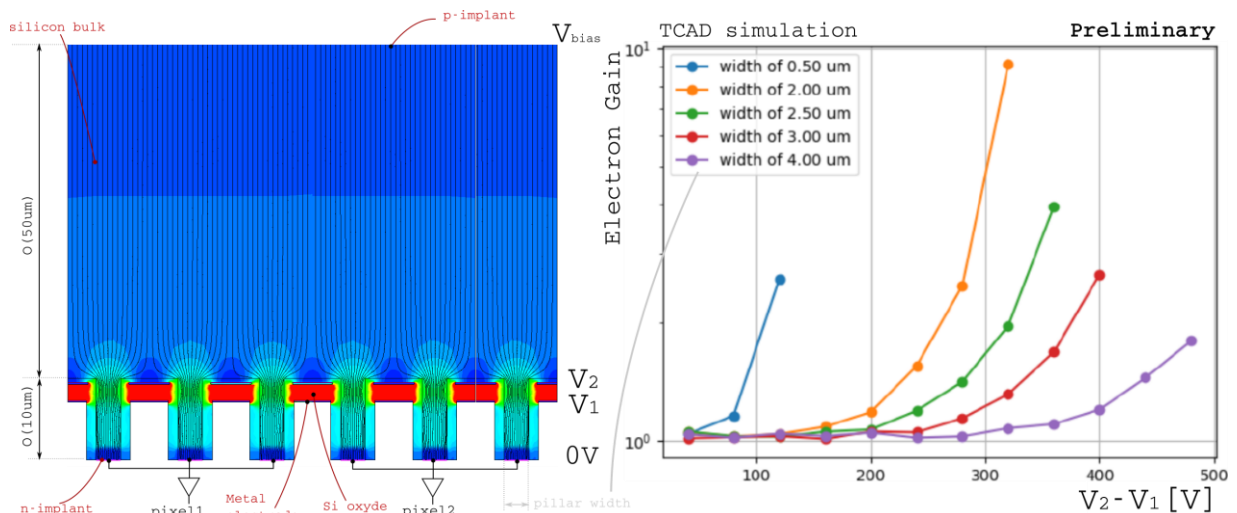


Figure 2: Active gain layer implant evolution with respect to radiation fluence for Boron [B], Gallium [Ga], and Boron+Carbon [B+C] (left) Gain reduction estimated through comparison of gain and non-gain regions of same die (right)

To further investigate defect engineering through **alternative implants**, the use of **Indium (In)** and **Lithium (Li)** for which promising results under electron and neutron irradiation have been reported [2,3], will be studied. In order to quantify their impact on radiation hardness, structures with identical active dopant profiles need to be produced. A detailed process simulation has been performed to determine the implantation parameter combination yielding an equivalent doping profile for B, Ga and In. More than 1000 different scenarios were explored for each implant type, varying the implantation energy, dose, diffusion time and screen oxide. The obtained profiles were compared in terms of penetration depth, integrated dose and form. The best scenario provides an 85% agreement in all three variables. A RD50 project has been prepared to implement those structures, including B, In, but also B+Li, In+Li and In+C co-implantation.

A new concept of sensor with intrinsic gain is also under investigation, named **Solid state Electron Multiplier (SSEM)** [4]. This design aims not only to mitigate radiation damage but also to improve on fill factor and segmentation with respect to LGADs. The amplification layer is obtained via a GEM-like metal structure embedded within the silicon bulk. Two fabrication approaches were examined, one using deep reactive ion etching and a second using wafer bonding. Their respective technical feasibility has been investigated with CEA-LETI and fabrication process R&D has been identified. The simplest, the etching approach, was selected for further studies. Its geometry is being optimised with TCAD simulations, also considering the technical limitations. A gain factor of about 10 at the readout electrode is seen in simulation and preliminary studies exhibit promising signal shapes that should provide time resolutions similar to those of LGADs. The amplification pillar pitch, of around  $10\mu\text{m}$ , defines the smaller pixel pitch achievable, but several pillars can be combined to achieve larger pixel pitches.



**Figure 3: Illustration of the SSEM geometry. The color illustrates the electric field distribution within the sensor. Field up to  $250\text{kV/cm}$  can be obtained in the center of  $2\mu\text{m}$  pillars when the ditched electrodes are biased (left). The gain, obtained from TCAD transient simulations, with respect to the pillar width and potential difference applied to the amplification electrodes (right). Gains up to 10 can be achieved before current runaway.**

## 2.2. Hybrid sensor simulation

Accurate simulations of charge propagation within the sensor and the impact of the readout electronics are important to guide the development, in particular when targeting timing applications. The modification of the behaviour with radiation should also be understood. The **time resolution with respect to the sensor thickness** for planar pixel and pad detectors has been studied [5] using Garfield++[6]. Emulation of the front end and timewalk correction have been studied as illustrated in Figure 4. Tools are now in place to benchmark against measurements performed on the R&D structures of the planar sensor, but also against extensive sensor data from the NA62 experiment, via a collaboration with CPPM. The **modification of the behaviour with radiation** will also be studied. A set of functions were developed to import charge carrier lifetime maps from TCAD into Garfield in order to perform those studies. In addition, a three-trap model validated by measurement of the LHCb Velo upgrade sensors is being tested against the five-trap model from the RD50 collaboration. These tools will be used to compare with irradiated sensor results.

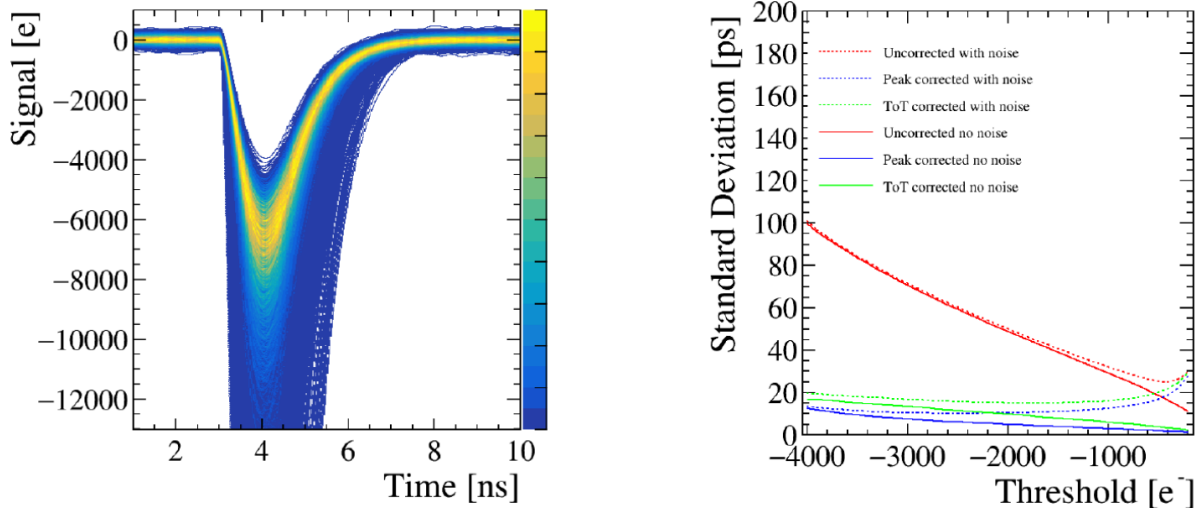


Figure 4: Simulated signal of a 110 $\mu\text{m}$  planar sensor readout by a fast shaper (left), the time resolution obtained at various thresholds from the sensor on the left, using various timewalk correction methods (right)

### 2.3. Fast and high-rate telescope and other timing setup

Work was done in 2020 to estimate the performance of a fast and high-rate **telescope based on Timepix4** readout with respect to other telescopes available or planned in the coming year. It was found to be the best option to qualify sensors targeting time resolution below 50ps, as the beamtime required by lower rate and/or lower timestamping capabilities telescopes becomes a limitation. This is illustrated in Figure 5. The construction of the telescope is due to start in 2021. It involves several institutes: CERN, Nikhef, USC, the University of Dortmund, the University of Oxford and IFCA. The work package is responsible for the mechanics and cooling of the telescope arms and DUT box. The conceptual design was done in 2020 and it will be constructed in the first half of 2021. In addition, the mechanics and cooling will be compatible with the EUDET telescope, to provide it with independent Timepix4 planes in the frame of an AIDA-innova project. The work package will also contribute to the telescope with the sensors (see 2.1), slow control and tracking and alignment software.

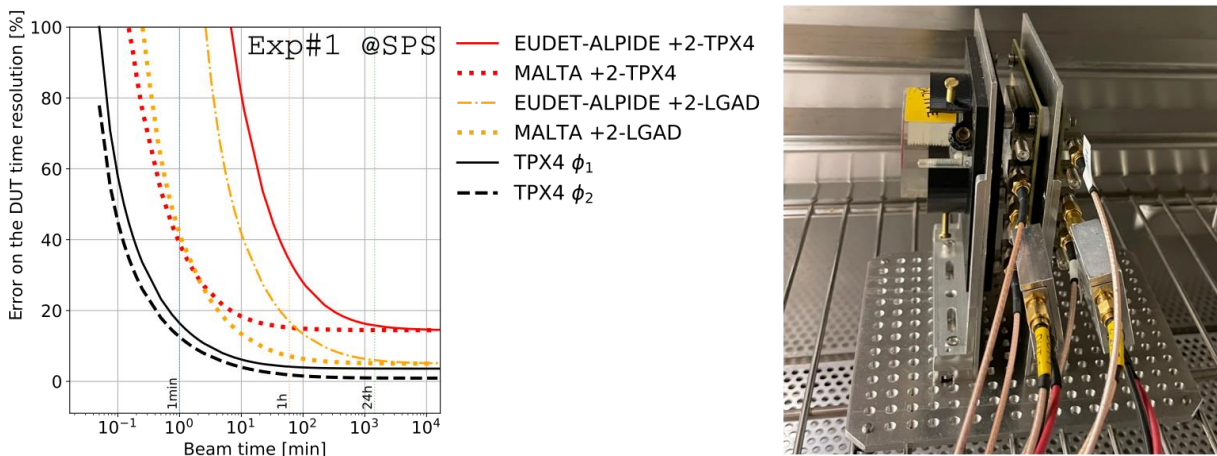


Figure 5: Comparison of the beam time needed by various telescope options to reach a given relative uncertainty on the measurement of the time resolution of individual 50 $\mu\text{m}$ x50 $\mu\text{m}$  pixel with 20ps time resolution for 10 high-voltage settings (left), the  $\beta$ -source setup in the climate chamber (right).

While telescopes provide the ultimate characterisation tools, a more available setup to test the many sensor structures that will be produced in the coming year is needed. The choice was made to use and further develop the  **$\beta$ -source setup** used for the LGAD studies. It consists of a <sup>90</sup>Sr beta source, followed by two sensor planes. A view of the setup placed in a climate chamber is shown in Figure 5, right.



Unsupervised remote operation allows to do temperature and voltage scans, and the analysis framework allows to evaluate a wide range of sensor properties from time resolutions down to 20-25ps to collected charge, dark rate or sensor efficiency including in low-gain and high-noise conditions. The setup and its analysis framework, which were developed by the work package fellow, are shared with the community and used in other institutes. Ongoing design modifications will allow to measure pixel edge efficiency and perform uniformity studies. To ensure penetration through all planes,  $\beta$ -particles at the higher energy tail will be selected via the integration of an electron monochromator. Finally, a multi-channel acquisition is under implementation for multi-pad and pixelated array timing performance evaluation.

#### 2.4. IC block design

The work on IC design will only start on 2021 with the hiring of a fellow. Specification from targeted applications (generic 4D tracking, LHCb upgrade 2, NA62 upgrade...) is being collected and discussed with the WP 5.

### 3. Publications and contributions to conferences and workshops

36th RD50 Workshop:

- Simulation of thickness dependence of time resolution for planar devices (M. Halvorsen)
- Acceptor removal and gain reduction in proton and neutron irradiated LGAD (V. Gkoukousis)

37th RD50 Workshop: :

- Comprehensive mip particle measurement and analyses system (V. Gkoukousis)
- Efficiency estimation on irradiated LGAD with respect to sensor stability (V. Gkoukousis)

ULTIMA 2020- Ultrafast Imaging and Tracking [**Canceled due to COVID**]

- Comprehensive technology study of radiation hard LGADs (V. Gkoukousis)

VERTEX /ICHEP

- Acceptor Removal study included in “Low Gain Avalanche Detectors for 4-dimensional tracking applications in severe radiation environments” - RD50 presentation

MASTER THESIS

- M. Halvorsen, “Optimisation of Silicon Pixel Sensors for Timing Applications”, Master thesis Norwegian University of Science and Technology (NTNU), CERN, 2020 [**To appear**]

### 4. References

---

- [1] E. Curras et. al. “Inverse Low Gain Avalanche Detectors (iLGADs) for precise tracking and timing applications” Nuclear Instrumentation Method A, [Volume 958](#), 162545 (2020)
- [2] D.J. Paez et. al. “Indium as a p-type dopant of thin film silicon solar cells”, Thin Solid Films Volume 615, 30 September 2016, Pages 358-365, <https://doi.org/10.1016/j.tsf.2016.07.053>
- [3] E. Oliviero et al., “Lithium implantation at low temperature in silicon for sharp buried amorphous layer formation and defect engineering”, Journal of Applied Physics 113, 083515 (2013); <https://doi.org/10.1063/1.4793507>
- [4] V. Coco, Solid State Electron Multiplier, Dec 2020: [https://indico.cern.ch/event/978916/contributions/4124124/attachments/2158600/3641472/20201208\\_WP1\\_1\\_EPRnD\\_SSEM.pdf](https://indico.cern.ch/event/978916/contributions/4124124/attachments/2158600/3641472/20201208_WP1_1_EPRnD_SSEM.pdf)
- [5] M. Halvorsen, “Optimisation of Silicon Pixel Sensors for Timing Applications”, Master thesis Norwegian University of Science and Technology (NTNU), CERN, 2020 [**To appear**]
- [5] H. Schindler, “Garfield++ User-Guide”, <https://garfieldpp.web.cern.ch/garfieldpp/documentation/UserGuide.pdf>

## WP1.2 Monolithic Silicon Pixel Detectors

### 1. Introduction

Monolithic pixel sensors receive increased interest due to their potential for tracking, timing, and even calorimetry in future high energy physics experiments. The EP R&D Work package for the development of monolithic CMOS Pixel sensors plans to address different classes of applications, with two already well identified: (A) Very high resolution vertex measurements requiring extremely low mass and hence low power, (B) vertex and tracking measurements in high rate and hostile environments at the HL-LHC, and others. The long term aim is to develop CMOS pixel sensors for future experiments in sub-100nm CMOS processes, if possible. Significant experience exists in the 180nm TowerJazz CMOS imaging technology with large scale production of ALPIDE [1] for the ALICE ITS2 upgrade ( $>10 \text{ m}^2$ ), process modifications for accelerated charge collection and radiation tolerance [2-6] applied for several experiments and in the EU funded STREAM and FASTPIX projects, and several submissions with strong contributions from external groups.

These developments are ultimately likely to use the same advanced CMOS technologies. The first technology identified is the 65 nm imaging flavor of TPSCo, the 65 nm ISC technology. TPSCo is a joint venture between TowerJazz and Panasonic. EP-ESE will provide access and support for the chosen technologies and aims to maximize synergies between the developments. A first MLR submission was completed end of last year in synergy with the ALICE experiment but with a strong contribution from groups inside and outside of ALICE, also financially.

Five fellows, one postdoc and five Ph.D. students are now active and directly associated with this work package. There was a Covid related delay in recruitment of about 4 months for some of the fellows and students. Several are financed directly by the EP R&D, some have been made available by the LCD group in the early stages, three by ALICE for the development (A). A significant effort to prepare testing for the 65 nm is now being provided by the groups in ALICE and the groups that have participated in the design. A very significant testing effort on the 180 nm with staff, fellows and students, continues to be provided by groups and institutes involved in development (B), CLICTD and FASTPIX. Synergies exist with several other work packages, for instance with WP1.4 for the development of test systems and simulation tools. Several activities are included in the AIDAInnova project.

### 2. Main activities and achievements in 2020

#### 2.1. Common technology evaluation and validation

The first MLR submission in the TPSCo 65nm ISC was completed with masks approved end 2020. Intense sensor design and process optimization continued in January with direct and regular contact with the foundry in Japan. The submission was in synergy with the ALICE experiment for the development of the ITS3 stitched sensor, with design contributions from groups in and outside ALICE: CPPM, DESY, IPHC, NIKHEF, STFC (RAL), Yonsei University (South Korea). The lot is expected back mid May. Fig. 1. shows a screenshot of the submitted designs. They include pixel test matrices, LVDS/CML receiver/driver, bandgaps, T-sensors, VCO, amplifiers, ring-oscillators, and transistor test structures.

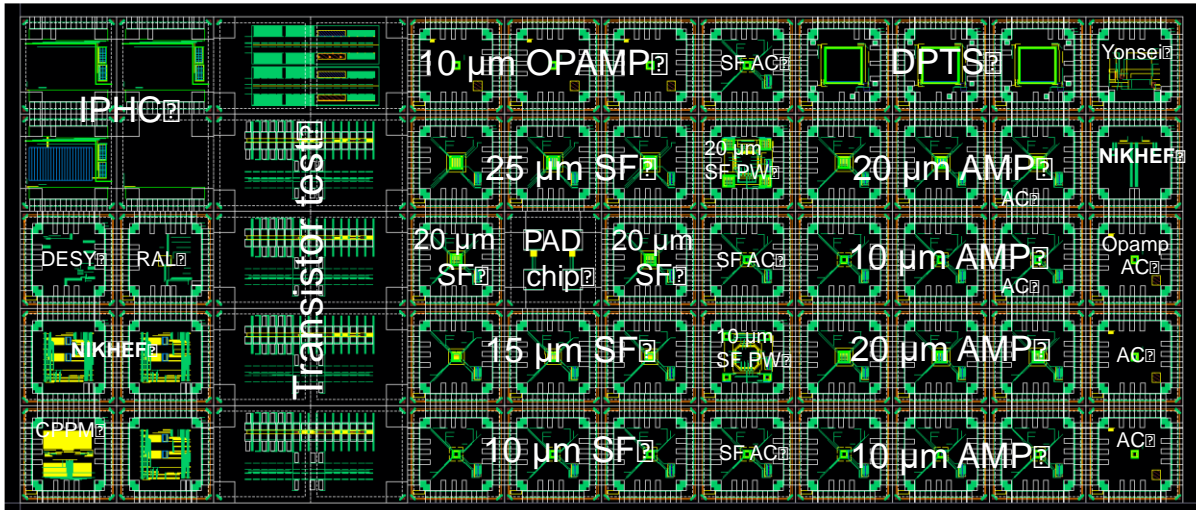


Fig. 1. Overview of the MLR submission in the TPSCo 65 nm ISC technology.

Design kit access for the TPSCo 65 nm was granted for several participating groups and a very good contact with the foundry was established, first with Israel, then directly with Japan, with meetings but also prompt detailed technical feedback upon request. Several new groups expressed interest to join. A new NDA and a collaboration agreement are being finalized for the further activities.

## 2.2. Submissions for fabrication in 180 nm

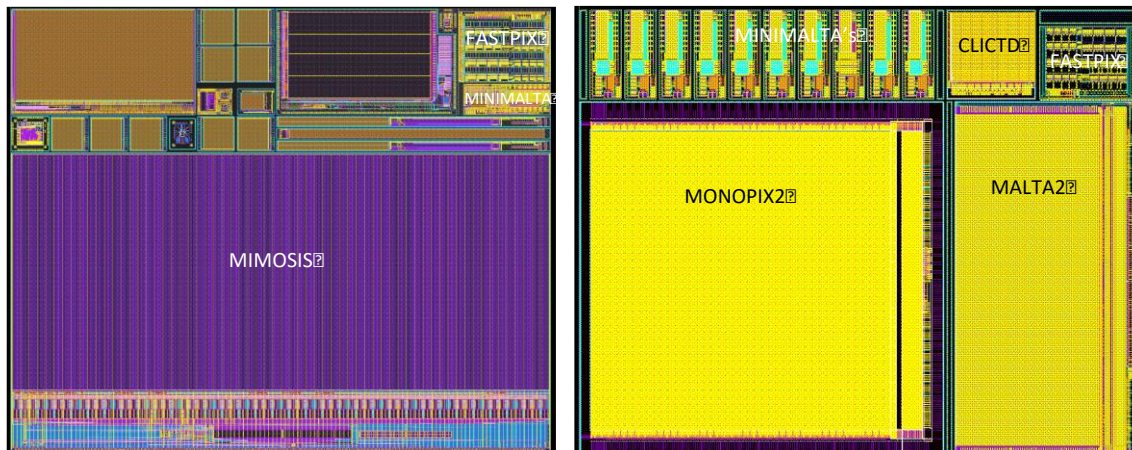


Fig. 2. Screenshot of the reticle of the two submissions in 180nm.

The first submission in 180 nm in 2020 took place in March and included the first MIMOSIS prototype and several other chips designed in an effort led by IPHC (Strasbourg), and the FASTPIX chip [5], designed by CERN in a EU-funded collaboration with INFN and Ritsumeikan University. The reticle also included a MiniMALTA chip [3]. The second submission in November included two large chips, MONOPIX2 and MALTA2, oriented towards development (B) and designed by Bonn University, CPPM, IRFU and CERN, and several MiniMALTAs, a CLICTD [4] and FASTPIX chip. Both submissions contained several process and sensor design splits, the first only on epitaxial material, the second also explored Czochralski (Cz) material after first encouraging results from a previous run. A MiniMALTA on the first run demonstrated a significant front end improvement guiding the front end modifications for the second run. Measurement results on MiniMALTA, CLICTD, and FASTPIX are further described below.

### 2.3. TCAD and Monte Carlo simulation

Significant sensor optimization using 3D finite element TCAD simulations was already carried out to accelerate the charge collection for sensors with small collection electrode in the 180nm TJ CMOS process [2]. As sensor radiation tolerance, time tagging precision and efficiency for thin sensors are simultaneously improved, this is relevant for many applications and already applied in MALTA, MONOPIX, CLICTD, FASTPIX, MIMOSIS and INVESTIGATOR chips, all fabricated in 180 nm. The same concepts have now also been used for the TPSCo 65nm ISC process in the first MLR run, where they have an even stronger impact to reduce charge sharing and guarantee fully efficient operation for a thinner sensor layer. The optimization now combines 3D TCAD and Allpix squared and Garfield++ Monte Carlo simulations.

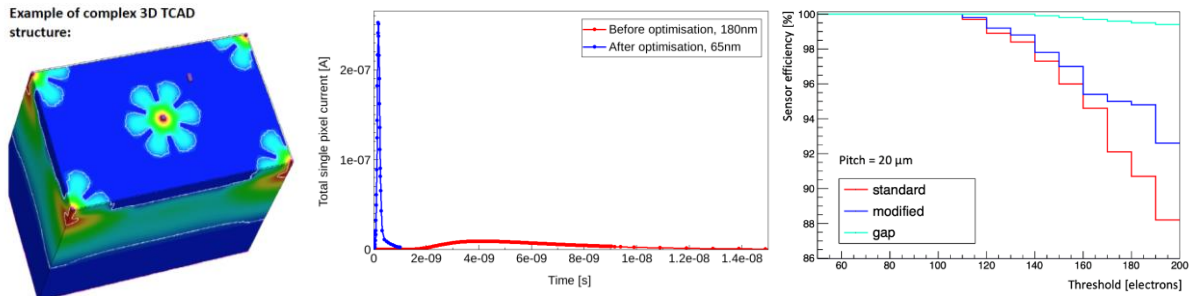


Fig. 3: electrostatic potential from complex 3D TCAD simulations (left), transient TCAD simulation before and after simulation based optimization (middle) and a Monte Carlo simulation result of detection efficiency of various flavors (right).

Fig. 3 shows an example of a 3D TCAD simulation with the collection electrodes placed in the center and edges of the structure with a complex optimized implant structure around them (left), a current pulse for a particle traversing the pixel cell at the pixel corner, the worst case scenario in view of charge collection speed (middle). Two current pulses are shown, before optimization in the 180nm process and after optimization in the 65nm process, illustrating an improvement of charge collection speed over several orders of magnitude. Increasing the collection speed improves radiation tolerance as signal charge is not as easily captured by radiation-induced traps. Fig. 3 (right) illustrates that the efficiency as a function of charge threshold for various sensor flavors is also affected, even prior to irradiation. The best has the highest collection speed. This Monte Carlo simulation provides statistics over a large number of particle incidences, randomized in position of incidence and generated charge, allowing a more precise determination of the final sensor performance compared to what can be achieved by computation intensive transient TCAD simulations. Further information can be found in the WP1.4 report.

### 2.4. 180 nm measurements

#### MiniMALTA & MALTA

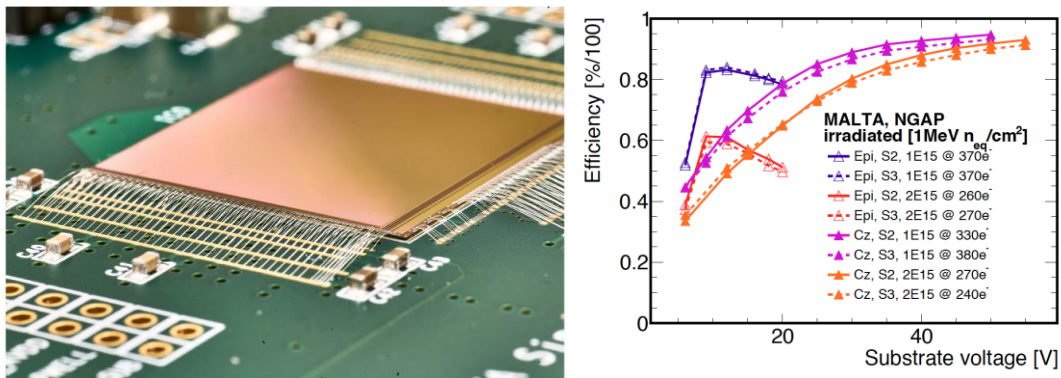


Fig.4. Picture of the MALTA chip and comparison of efficiency after an irradiation of  $2E15 n_{eq}/cm^2$ .



The MONOPIX and MALTA chips were developed within the STREAM project aiming application in the outer pixel layers of the ATLAS high-luminosity upgrade. MONOPIX uses a synchronous architecture, and MALTA with a  $2 \times 2 \text{ cm}^2$  pixel matrix with  $512 \times 512$  pixels of  $36.4 \mu\text{m} \times 36.4 \mu\text{m}$ , an asynchronous readout architecture. Full sensor depletion for a small collection electrode is achieved via a deep low dose n-type implant. Further sensor improvements accelerate the signal charge towards the collection electrode to bring radiation tolerance in the  $1\text{E}15 \text{ n}_{\text{eq}}/\text{cm}^2$  realm. Several runs were carried out earlier and also Cz material was included in the later runs. Fig. 4 shows a picture of the MALTA chip and recent measurements after  $2\text{E}15 \text{ n}_{\text{eq}}/\text{cm}^2$  where with increasing reverse bias the sensors in Cz material become more efficient due to further depletion into the substrate and hence a larger signal.

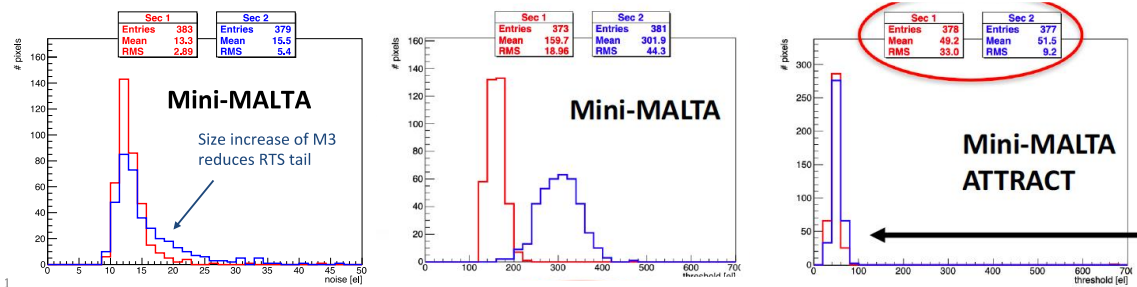


Fig.5. A size increase of the main NMOS in the MALTA front end yields lower RTS noise (left), and better threshold uniformity (middle). Cascoding this transistor for further gain enhancement significantly improves threshold uniformity (right).

In this measurement, the efficiency of the MALTA chip is still heavily affected by random telegraph noise (RTN or RTS) and a relatively large output conductance of the main NMOS transistor in the front end adversely affecting the signal gain. A measurement on MiniMALTA, a small demonstrator chip derived from MALTA, showed that a size increase of this NMOS transistor reduced its RTS noise and increased the gain. This is illustrated in fig. 5, comparing noise (left) and threshold (middle) distributions before and after the size increase. Another front end improvement, cascoding this NMOS transistor to further enhance the gain, included on a MiniMALTA on the March FASTPIX/MIMOSIS run, significantly improves charge threshold uniformity and margin for operation at low thresholds as illustrated in Fig. 5 (right). These measurement results were then used to guide the modifications of the front end in MALTA2.

#### CLICTD

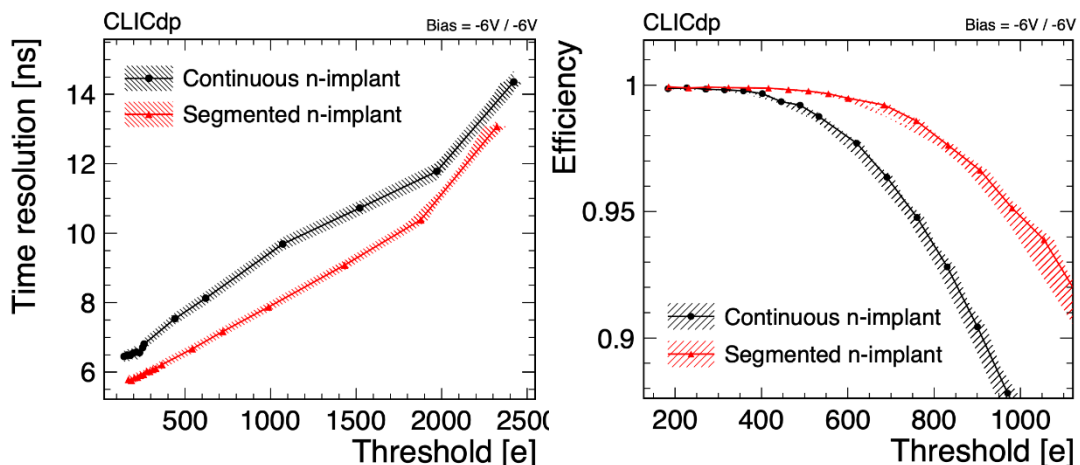


Fig.6. Time resolution (left) and efficiency (right) as a function of threshold for the two pixel flavors in the CLICTD sensor.

The CLICTD sensor is a technology demonstrator for the 180nm TJ pixel designs, targeting the requirements of large-area tracking detectors for future Higgs factories. Its pixel matrix consists of  $16 \times 128$  detection channels measuring  $300 \mu\text{m} \times 30 \mu\text{m}$ . Each channel is segmented into 8 sub-pixels with

individual collection electrodes in order to reduce the amount of digital circuitry while maintaining a small sub-pixel pitch.

In 2020, CLICTD was characterized in several successful test-beam campaigns. The results allow for a detailed comparison of the 180nm TJ pixel flavors.

On the left of Fig. 6, the time resolution as a function of threshold for two different pixel flavors is shown. The flavor with the segmented n-implant was optimized for fast charge collection and therefore exhibits a better time resolution. The faster charge collection also affects the detection efficiency, shown on the right of Fig 6. Charge sharing is suppressed for the pixel flavor with segmented n-implant leading to a higher seed signal and therefore to a wider threshold range, where the sensor is fully efficient.

### FASTPIX

After the process modifications for full depletion of the sensitive layer, and adaptations for CLIC and ATLAS, the FASTPIX project was started for further timing improvements. The FASTPIX prototype is equipped with 32 pixel matrices, each with 4 pixels connected to a fast analog output and 64 pixels read out digitally. Pixel pitches are 8.66, 10, 15 and 20  $\mu\text{m}$ , collection electrodes are placed on a hexagonal grid.

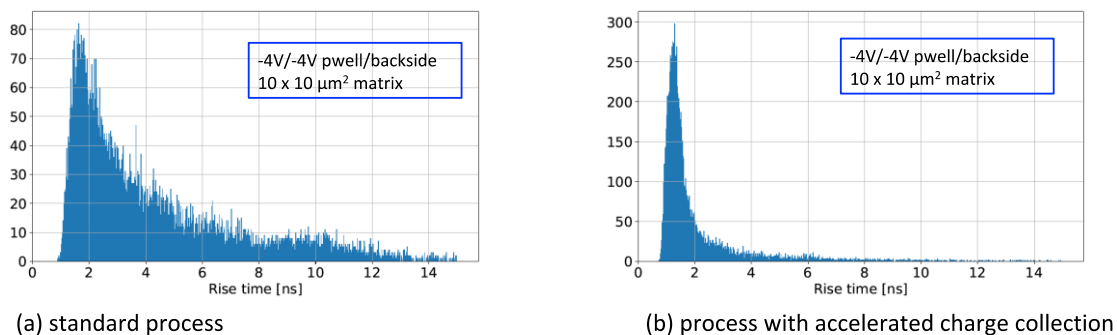


Fig. 7. 20-80 % rise time distributions obtained with the  $^{90}\text{Sr}$  source, (a) standard and (b) modified process.

When illuminating the chip with a  $^{90}\text{Sr}$  source, pulses were observed on both analog and digital outputs, confirming functionality of the sensor and on-chip circuitry. Fig. 7. compares 20-80% rise time distributions of the signals on the analogue outputs for two flavors of the prototype chip, one with no additional measures to accelerate the collection of signal charge (standard process), and another one with several modifications to increase the electric field pushing the signal charge in the sensor towards the collection electrode (modified process). The improvement is evident, demonstrating the validity of the methods to accelerate the charge collection, even for pixel pitches as low as 10  $\mu\text{m}$ . This gives confidence that the same techniques could yield even better performance in 65 nm. Further tests are in progress also on a laser test setup for further time resolution studies.

### 3. Publications and contributions to conferences and workshops

#### SIMULATIONS

##### Journals

- Simon Spannagel et al., Combining TCAD and Monte Carlo methods to simulate CMOS pixel sensors with a small collection electrode using the Allpix2 framework, NIM 964 (2020) 163784.

## Conferences/talks

- Paul Schuetze et al., What's new on Allpix Squared?, Beam Telescopes and Test Beams Workshop 2021
- Magdalena Munker, Fast charge collection in small collection electrode monolithic CMOS sensors, CERN Detector Seminar January 2021, <https://indico.cern.ch/event/997569/>

## MALTA & MiniMALTA

### Journals

- H. Pernegger et al., Radiation hard monolithic CMOS sensors with small electrodes for High Luminosity LHC, 2021 NIM A 986 164381
- L. Flores et al Design of large scale sensors in 180 nm CMOS process modified for radiation tolerance, 2020 NIM A 980 164403
- M. Dyndal et al., Mini-MALTA: radiation hard pixel designs for small-electrode monolithic CMOS sensors for the High Luminosity LHC, 2020 JINST 15 P02005

### Conferences

- F. Dachs et al., Comparative study of MALTA pixel detectors on epitaxial and Czochralski silicon, TREDI 2021
- A. Gabrielli et al., MALTA CMOS sensor telescope: new developments and recent measurements, 9<sup>th</sup> Beam Telescopes and Test Beams Workshop 2021
- I. Asensi et al., Latest developments and results of radiation tolerance CMOS sensors with small collection electrodes, VERTEX 2020
- C. Solans et al., Radiation hard monolithic CMOS sensors with small collection electrodes for the HL-LHC and beyond, ICHEP 2020

## CLICTD

### Journals

- Kremastiotis et al., Design and Characterization of the CLICTD Pixelated Monolithic Sensor Chip, IEEE Trans.Nucl.Sci. 67 (2020) 10, 2263.
- R. Ballabriga et al., Test-beam characterisation of the CLICTD technology demonstrator - a small collection electrode High-Resistivity CMOS pixel sensor with simultaneous time and energy measurement, 2020, CLICdp-Pub-2021-001

### Conferences

- K. Dort, The CLICTD Monolithic CMOS Sensor, proceedings of the [29th International Workshop on Vertex Detectors](#), 2020, CLICdp-Conf-2020-007.
- Dominik Dannheim et al., The CLICTD monolithic CMOS sensor for the CLIC tracking detector, TREDI 2020, <https://indico.cern.ch/event/813597/contributions/3730879/>

## FASTPIX:

- T. Kugathasan et al., Monolithic CMOS sensors for sub-nanosecond timing, NIM A 979 (2020) 164461.
- W. Snoeys et al., FASTPIX: sub-nanosecond radiation tolerant CMOS pixel sensors, ATTRACT Final Conference 2020, <https://attract-eu.com/wp-content/uploads/2019/05/FASTPIX.pdf>

---

[1] G. Aglieri Rinella et al. NIM A 845 (2017), p. 583-587, <https://doi.org/10.1016/j.nima.2016.05.016>

[2] W. Snoeys et al., NIM A 871 (2020), p. 90-96, <https://doi.org/10.1016/j.nima.2017.07.046>

[2] M. Munker et al., JINST 14, (2019), 05, C05013, <https://doi.org/10.1088/1748-0221/14/05/c05013>

[3] M. Dyndal et al., JINST, Vol 15, February 2020, <https://doi.org/10.1088/1748-0221/15/02/P02005>

[4] I. Kremastiotis et al., IEEE Tran. Nucl. Sci. (2020) 10, <https://doi.org/10.1109/TNS.2020.3019887>

[5] T. Kugathasan et al., NIM A 979 (2020), <https://doi.org/10.1016/j.nima.2020.154461>

## WP1.3 Silicon Modules

### 1. Introduction

Work package 1.3 focusses on the study and development of new modules for hybrid and CMOS pixel detectors. The activities can be grouped into four main areas:

- Study of enabling technologies (interconnection, post processing, packaging)
- Building of demonstrator modules
- Testing and qualification of components as well as demonstrator modules
- QC procedures and infrastructure for modules and components

Working closely with industrial suppliers as well as with CERN services (e.g. the EP-PCB workshop) is an important aspect of the activities. In addition to work package meetings, topical meetings have been organised throughout 2020, with invited speakers that introduce specific topics (e.g. Ni/Au plating at CERN, encapsulation studies, Parylene coating).

Synergies are explored not only with other work packages (e.g. 1.2 and 1.4) but also with outside groups (e.g. from University of Calgary) as well as within international collaborations such as AIDAInnova. Several staff members, a project associate (R. Cardella, until August 2020), a fellow (M. Vincente Barreto Pinto) and a doctoral student (M. Williams) have been involved in the WP 1.3 activities from the beginning of 2020. In October 2020 one doctoral student (M. van Rijnbach) and one fellow (F. Dachs) joined the work package.

### 2. Main activities and achievements in 2020

In 2020 the activities have focused on the study of enabling technologies and the assembly and building of demonstrator modules while also first tests of modules could be carried out. The following sections will provide a summary of these activities.

#### 2.1. Thinning and Dicing studies

Wafer thinning to 100-micron thickness and laser dicing has been carried out by DISCO Germany using STREAM2 wafers. The STREAM2 wafers contain MALTA2 and MONOPIX2 monolithic silicon pixel chips as well as several smaller prototype chips. The use of laser dicing allows to reduce the inactive area outside the pixel chip to a few microns. Earlier tests carried out on STREAM1 wafers [1] have shown excellent dicing edge qualities and indicated an increased substrate breakdown voltage for MALTA1 chips [2] diced with laser compared to blade diced chips (see Figure 1). In the following a systematic study of the MALTA2 chips will be carried out and compared to earlier results.

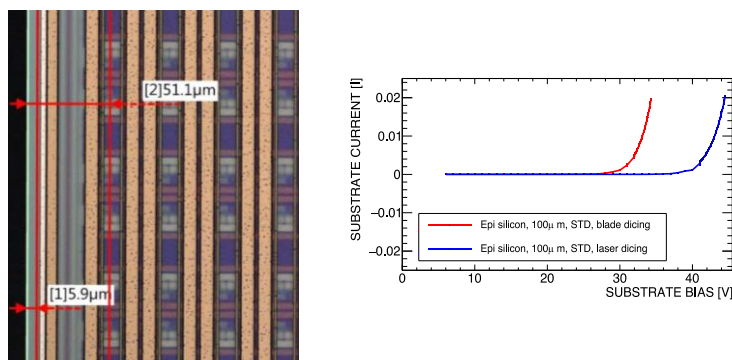


Figure 1: Microscope image of a laser diced MALTA1 chip edge with the dicing cut at 5.9 microns from the seal-ring (left) and substrate I-V curves for laser and blade diced MALTA1 chips (right) showing an increased breakdown voltage for the laser diced sample.

Thinning of individual dies has been performed by Optim Wafer Services (Greasque, France) for CLICTD monolithic pixel sensors (down to 40, 50 and 100 micron thickness) and for FASTpix monolithic timing demonstrators (down to 50 micron thickness). A good thinning yield of 80-90% has been achieved, and the resulting assemblies are characterised with ongoing laboratory and test-beam measurements [3].

### 2.2. Hybridisation with fine-pitch bump bonding

A 25-micron-pitch single-die hybridisation process using SnAg solder bumps is under development with IZM (Berlin) [3,4]. The project uses CLICpix2 ASICs with 300-micron thickness and planar active-edge sensors from Advacam and FBK with 50-150 micron thickness.

In the first phase of the project, concluded in 2020, a total of 9 assemblies has been produced and characterised in detail, using optical inspection techniques (Figure 2), as well as electrical and test-beam measurements. The interconnect quality for seven electrically functioning assemblies is quantified using a data-driven pixel categorisation scheme (Figure 3). High interconnect qualities are achieved for two assemblies, with yields of up to 99.6%. The characterisation results have been used to optimise the solder bump-bonding process.

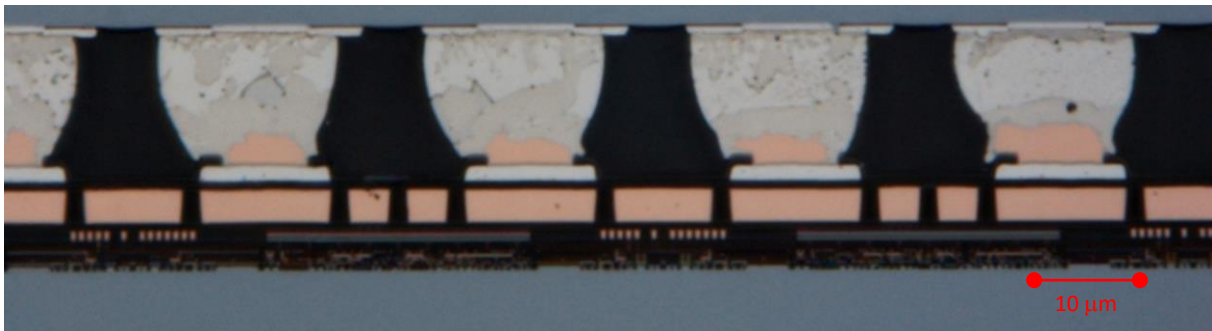


Figure 2: Cross section through solder bumps in CLICpix2 assembly (Image credit: Fraunhofer IZM).

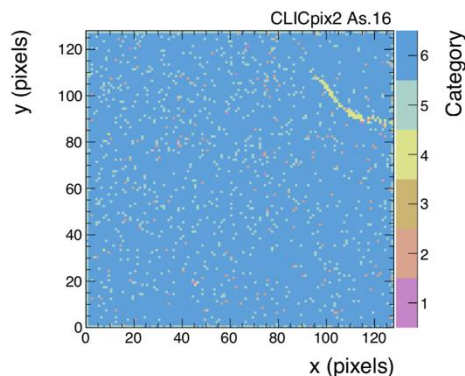


Figure 3: Pixel categorisation results for a CLICpix2 assembly with FBK sensor. Categories: 1=masked due to noise, 2=unresponsive to test pulsing, 3=shorted, 4=bonding/sensor issue, 5=high-rate, 6=expected response.

The ongoing second phase of the project aims at demonstrating an improved yield of high-quality assemblies, using optimised processing parameters and active-edge sensors from a recent FBK AIDA-2020 production with thicknesses from 50 to 130 microns.

### 2.3. Hybridisation and module integration with Anisotropic Conductive Film (ACF)

An alternative in-house pixel-detector hybridization technology based on Anisotropic Conductive Films (ACF) with micro particles embedded in resin is under development with industrial partners (Conpart and Dexerials), to replace the conventional costly fine-pitch flip-chip bump bonding [5,6] (Figure 4 left). It can also be used for the integration of hybrid or monolithic detectors in modules, replacing wire bonding or solder bumping techniques.



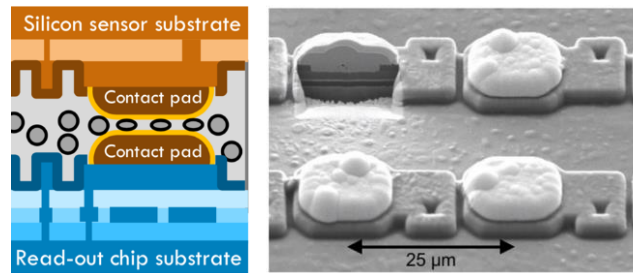


Figure 4: Left: Schematic representation of ACF hybridisation with micro-particles between sensor and readout ASIC. Right: ENIG plated pixel pads on CLICpix2 ASIC.

An automatic component placer (flip-chip machine) at University of Geneva is used for the in-house production of ACF assemblies and for the optimisation of process parameters and assembly techniques. The pixel pads are either metallized on wafer level in an industrial Electroless Nickel Electroless Palladium Immersion Gold (ENEPIG) plating process, or on single-die level using an Electroless Nickel Immersion Gold (ENIG) plating process developed in EP-DT-EF (Figure 4 right).

Functional hybrid-detector assemblies have been produced with 55-micron pitch planar pixel sensors bonded to Timepix3 readout ASICs. Device cross sections and measurements with radioactive sources have been performed, showing an interconnect coverage of up to approximately 1 cm<sup>2</sup> corresponding to a connection yield of about 50% (Figure 5). Future work will focus on improving the coverage by further optimisation of the bonding parameters and using improved ACF material (e.g. thinner adhesive layers, aligned micro particles). Additional bonding tests are planned for 25-micron pitch CLICpix2 hybrid assemblies.

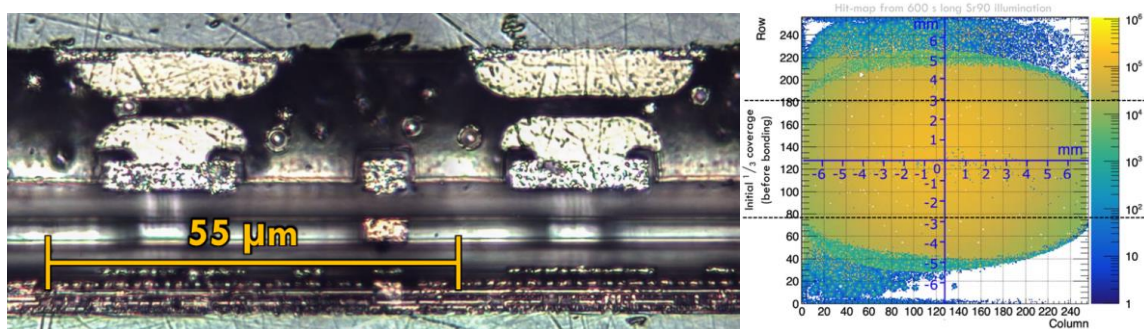


Figure 5: Left: Cross section through Timepix3 ACF assembly (sensor on top). Right: Hit map from Sr-90 source exposition on Timepix3 ACF assembly. The oval region with high hit rates corresponds to the partial coverage of the ACF tape on the matrix.

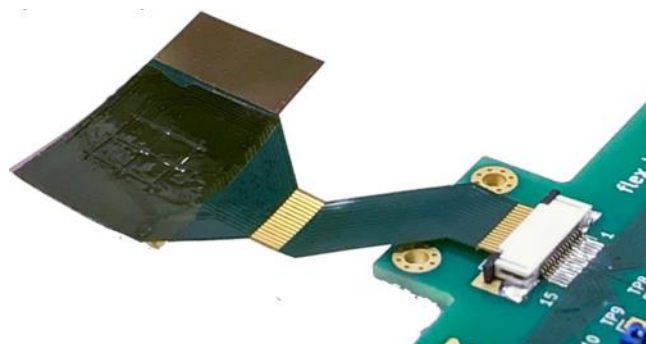


Figure 6: ALPIDE-on-flex assembly after ACF bonding.

Recently the ACF studies have been extended towards interconnections of 50-micron thin ALPIDE monolithic sensors to flexible PCBs, using a redistribution metal layer and bonding pads on the chip

surface. First functional samples have been produced (Figure 6), and measurements show very low contact resistances (<1 Ohm), nominal power consumption and fully functional sensors.

Mechanical and ageing tests are ongoing to confirm the flexibility and robustness of the assemblies. Future work aims at building larger modules with seamless tiling of sensors (<20 micron gaps). ACF interconnect studies are also planned for chip-to-chip interconnections of monolithic MALTA sensors using silicon interposers, as described in the following section.

#### 2.4. Multi-chip module studies and test

MALTA monolithic pixel chips are used to develop a radiation hard, large area and light weight pixel module. The MALTA chip was designed with chip-to-chip powering and communication pads on both sides of the pixel matrix. Each chip includes 40 CMOS transceivers which can be used for chip-to-chip data transmission with a pulse width of 1 ns.

The data transfer from one MALTA chip to another (Figure 7 left) has been successfully demonstrated using ultrasonic Al wedge wire bonds between the two chips (Figure 7 right). Source tests using Sr90 and Fe55 sources have been used to demonstrate the correct data transfer from one chip to another [7, 8].

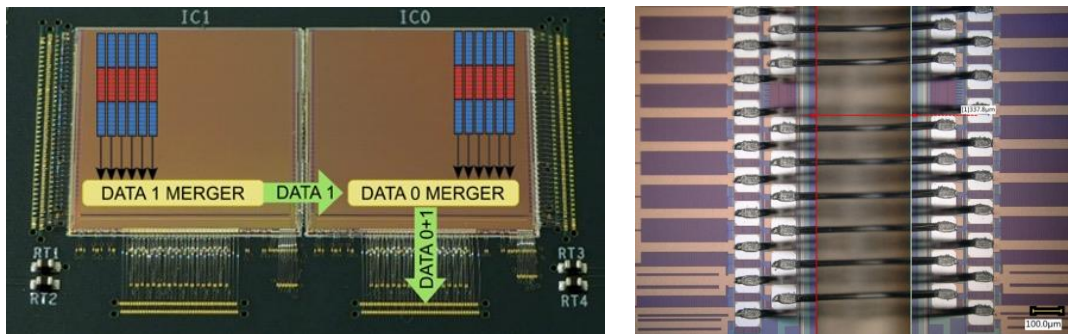


Figure 7: Left: Al wedge wire bonds between two MALTA chips for data and power transfer. Right: Schematic view of the data transfer and merging between two MALTA chips.

Ongoing studies explore alternatives to wire bonding that will also provide a mechanical support, such as a silicon-bridge and ACF bonding. An example of two MALTA chips (100 micron thick) connected with a silicon bridge can be seen in Figure 8 (left). The connections between the silicon bridge and the MALTA chips has been realized using SnAg-capped Cu studs (Figure 8 right).

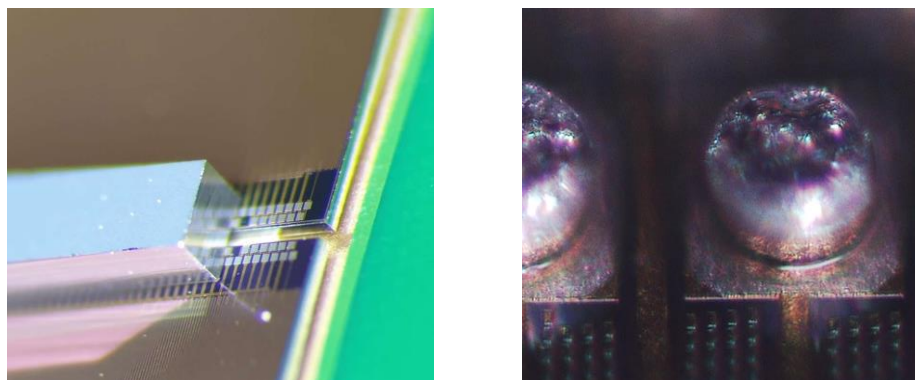


Figure 8: Left: Two MALTA chips connected using a Si-bridge structure. Each pad on one chip is connected to the corresponding pad on the other chip by flip chip connecting the silicon bridge. Right: Microscope image of a Cu/SnAg connection on the silicon bridge (diameter 60 microns).

A dedicated PCB to test the data transfer between four MALTA chips has been designed and produced and first chips are currently being mounted and tested.

### 3. Publications and contributions to conferences and workshops

#### Conference contributions:

- K. Dort, "The CLICTD Monolithic CMOS Sensor ", 29th International Workshop on Vertex Detectors, Japan, 2020
- M. Vicente Barreto Pinto, "Novel hybrid pixel detectors", 4th FCC Physics and Experiments Workshop, 2020 (online)
- F. Dachs et al., "Comparative study of MALTA pixel detectors on epitaxial and Czochralski silicon", 16th Trento workshop on advanced silicon radiation detectors 2021 (online)
- M. Vicente Barreto Pinto, "Pixel detector hybridization and integration with Anisotropic Conductive Films", 16<sup>th</sup> Trento workshop on advanced silicon radiation detectors 2021 (online)
- P. Riedler, "Interconnection studies for monolithic silicon pixel detector modules using the MALTA CMOS pixel chip", 16<sup>th</sup> Trento workshop on advanced silicon radiation detectors 2021 (online)

#### Publications:

- K. Dort, "The CLICTD Monolithic CMOS Sensor," in proceedings of the 29th International Workshop on Vertex Detectors, CLICdp-Conf-2020-007, Japan, 5 - 8 Oct 2020.
- M. Williams, "R&D for the CLIC vertex and tracking detectors," JINST, vol. 15 C03045, 2020.
- P. Riedler et al., "Studies for low mass, large area monolithic silicon pixel detector modules using the MALTA CMOS pixel chip", NIMA 990 (2021), <https://doi.org/10.1016/j.nima.2020.164895>

#### PhD thesis:

- M. Williams, Evaluation of Fine-Pitch Hybrid Silicon Pixel Detector Prototypes for the CLIC Vertex Detector in Laboratory and Test-Beam Measurements, PhD thesis, Univ. Glasgow, to appear 2021.

#### References:

- 
- [1] P. Riedler et al., "Studies for low mass, large area monolithic silicon pixel detector modules using the MALTA CMOS pixel chip", NIMA 990 (2021), <https://doi.org/10.1016/j.nima.2020.164895>
  - [2] F. Dachs et al., "Comparative study of MALTA pixel detectors on epitaxial and Czochralski silicon", 16th Trento Workshop on Advanced Silicon Radiation Detectors, 2021, <https://indico.cern.ch/event/983068/contributions/4223228/>
  - [3] K. Dort, "The CLICTD Monolithic CMOS Sensor," in proceedings of the 29th International Workshop on Vertex Detectors, CLICdp-Conf-2020-007, Japan, 5 - 8 Oct 2020.
  - [4] M. Williams, "R&D for the CLIC vertex and tracking detectors," JINST, vol. 15 C03045, 2020.
  - [5] M. Williams, Evaluation of Fine-Pitch Hybrid Silicon Pixel Detector Prototypes for the CLIC Vertex Detector in Laboratory and Test-Beam Measurements, PhD thesis, Univ. Glasgow, to appear 2021.
  - [6] M. Vicente, "Novel hybrid pixel detectors," talk presented at the 4th FCC Physics and Experiments Workshop, 2020, <https://indico.cern.ch/event/932973/contributions/4102452/>.
  - [7] M. Vicente Barreto Pinto, "Pixel detector hybridization and integration with Anisotropic Conductive Films," 16th "Trento" Workshop on Advanced Silicon Radiation Detectors, 2021, <https://indico.cern.ch/event/983068/contributions/4223158/>
  - [8] P. Riedler, "Interconnection studies for monolithic silicon pixel detector modules using the MALTA CMOS pixel chip", 16th Trento Workshop on Advanced Silicon Radiation Detectors, 2021, <https://indico.cern.ch/event/983068/contributions/4223151/>

## WP1.4 Silicon Detectors – Characterization and Simulation

### 1. Introduction

This WP aims for enabling a fundamental understanding and optimization of the performance of particle detectors. The increasingly complex sensors and readout ASICs require improved



characterization techniques, detailed modelling and simulations and a better understanding of radiation effects up to the radiation levels expected at future hadron colliders. Most WP activities are building upon previously existing R&D activities, are performed in close collaboration with the other silicon WPs and are embedded in international R&D efforts like e.g. RD50, LHC-upgrades and CLICdp. The core resources provided by the EP-RD program for 2020 were one Fellow and one PhD student, which were largely extended by (part-time) Fellows and students from other funding sources at CERN and in collaboration with external institutes. From April 2021 onward most of the WP activities will be pursued also within the AIDAInnova project frame (Caribou, TPA-TCT, detector modelling, radiation damage studies, radiation monitoring and LGAD).

## 2. Main activities and achievements in 2020

### 2.1. Characterization Tools

Silicon detector characterization techniques and readout tools are being developed within WP1.4. The focus in 2020 was on the Caribou DAQ and the TPA-TCT technique and system which are described in more detail below. Improvements on the defect spectroscopy equipment is presented in section 2.2.

**Caribou** [1] is a flexible open-source DAQ system designed for laboratory and high-rate beam tests and easy integration of new detector prototypes developed within the EP-RD silicon work packages. It uses common hardware, firmware and software components that can be shared across different projects, thereby reducing the effort necessary to support new prototypes. Caribou is developed and maintained as a collaborative effort within the EP-RD WP 1.4 and the RD50

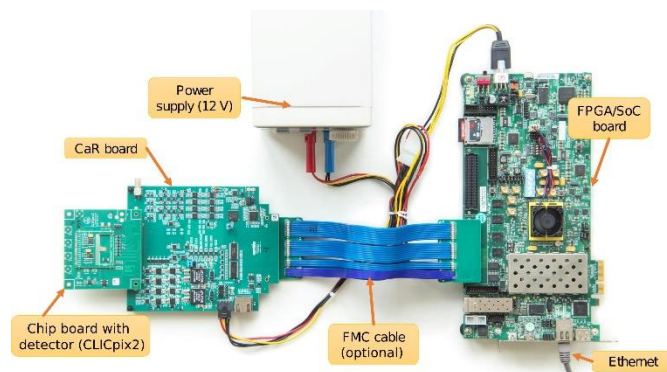


Figure 7. Caribou setup for laboratory measurements.

collaboration. It is part of the AIDAInnova project and supported by the RD50 common fund. The common hardware is mainly developed at BNL, while CERN and DESY are the main contributors to the common firmware and software. The system consists of a Xilinx Zynq System-on-Chip (SoC) board that runs the Peary DAQ software and detector-specific firmware, and the Control and Readout (CaR) board, which contains programmable power supplies, current sources, ADCs and DACs, clocks, and communication interfaces, and is connected to an application-specific chip-board that interfaces with the detector (Figure 7). A new hardware revision (1.4) of the CaR board with improved configurable power supplies was recently released. Support for the new revision was added to Peary and a batch of 20 new CaR boards was produced and distributed by the CERN EP-RD WP 1.4 team to the participating RD50 institutes after testing. Several test beam campaigns using Caribou were performed at DESY for CLICpix2 [2], CLICTD [3] and ATLASPix2 [4] detector assemblies. Caribou is currently also being used for readout of the ATTRACT FASTpix chip, which is a monolithic CMOS pixel sensor designed for sub-nanosecond timing. For this, a high-bandwidth oscilloscope is connected to the analog or digital outputs of the chip and waveforms are recorded by Peary over the network for later analysis. This successful integration of the FASTpix sensor in Caribou will serve as a template for the integration of the new monolithic test chips produced in the recent 65nm MLR submission in WP 1.2.

The **Two-Photon-Absorption Transient-Current-Technique (TPA-TCT)** uses laser pulses to excite charge carriers in silicon detectors. The resulting transient current is recorded to measure the charge collection efficiency, the electric field profile and other characteristics of the device under test. The particularity of TPA-TCT is the use of a femtosecond-laser with an emission wavelength corresponding

to a photon energy of less than the silicon band-gap. Two photons are necessary to create one electron-hole pair. The use of strong focusing optics allows reducing the volume in which charge carriers are generated to about  $1\ \mu\text{m}$  in the plane perpendicular to the beam and  $10\ \mu\text{m}$  along the beam propagation direction. Since 2019 a table top setup is under development in the Solid State Detector laboratory, the first of its kind in the world [5, 6]. The project received a seed funding from the CERN Knowledge Transfer fund and now continues in the framework of the EP-RD program. In the first 18 months of development, after initial successful tests, several technical difficulties occurred, which were solved in close collaboration with the laser supplier, but required a complete re-design of the laser. In early 2021 the laser arrived back to CERN after an upgrade at the suppliers premises increasing the power and spectral stability. Independently, at CERN, methods were developed to correct for power fluctuations of the laser source by either using two-photon absorption in a reference sensor or the second harmonic generation (SHG) in a BBO crystal. To position the sensor under test precisely and to correct any tilt of the detector surface with respect to the incident beam a high precision 6-axis motion controller is used. First successful measurements have been performed (see Figure 8 ) proving the high spatial precision of this technique and especially the possibility to perform 3D measurements. The increased stability resulting from the laser upgrade and the non-linear reference signal (TPA or SHG) has been verified. Work is ongoing on subcomponents of the system like the cooling stage that is supposed to cool down to  $-20^\circ\text{C}$  and an infrared camera system.

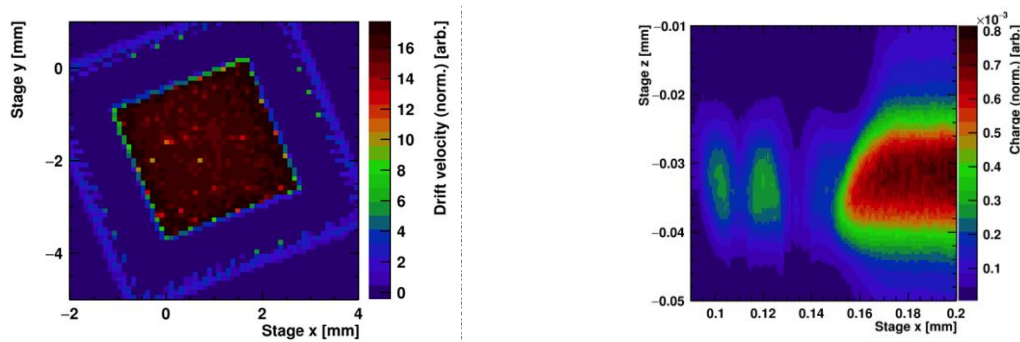


Figure 8. (a) 2D scan of the drift velocity in a Pad detector after tilt correction. The positioning systems allows rotations in all directions to scan along arbitrary axes.

(b) Collected charge as a function of depth and distance from the sensors edge in the peripheral region of an LGAD sensor. The active detector volume and fields close to the p-stop ring are clearly visible.

## 2.2. Radiation-damage studies and damage models

Silicon detectors operating in the high radiation field environment of the LHC experiments undergo a degradation in their performance that can be traced back to the interaction of the highly energetic particles with the sensor silicon atoms. This interaction leads to displacement of lattice atoms and the formation of point and cluster defects inside the sensor bulk that on the macroscopic side become visible e.g. in changes of leakage current, depletion voltage or charge collection efficiency. The type and amount of produced displacement defects is strongly dependent on particle type as well as particle energy and fluence. However, the impact of the defects themselves on the macroscopic detector performance should be independent of the particle types. Within this WP the formation of defects in p-type silicon devices that are responsible for the radiation-induced loss of amplification gain in high precision timing sensors (LGADs) for the CMS ETL and ATLAS HGTD detectors are studied with the aim to produce reliable damage predictions and develop defect engineering approaches to increase radiation hardness. Focus in 2020 was on high-energy electron and proton induced defect studies, which were conducted also in view of measuring the Non Ionizing Energy Loss (NIEL) scaling of the observed damage. The measurements will form the basis for the anticipated modelling approaches.

A **defect characterization campaign on electron irradiated p-type silicon sensors** was launched to complement previous studies on proton and neutron irradiated sensors [7, 8]. A series of p-type Si-

detectors (10  $\Omega$ cm to 1k $\Omega$ cm resistivity) was irradiated by electrons with energies of 5.5 MeV and up to 200 MeV, with the latter irradiation performed at the CLEAR electron accelerator at CERN. Changes in the effective carrier concentration of the sensors were extracted from capacitance measurements  $C(V)$  and reveal a decrease in  $N_{eff}$  after irradiation. Deep-Level-Transient-Spectroscopy (DLTS) and Thermally-Stimulated-Current (TSC) measurements were performed for defect identification. An example is given in Figure 9 (a), where DLTS spectra obtained on 10  $\Omega$ cm Si sensors irradiated with 5.5 MeV and 200 MeV electrons are shown, including data obtained after an annealing step and showing the transformation of the  $C_i$  defects into the  $C_iO_i$  defects as well as the decrease of  $B_iO_i$  defects with annealing time.

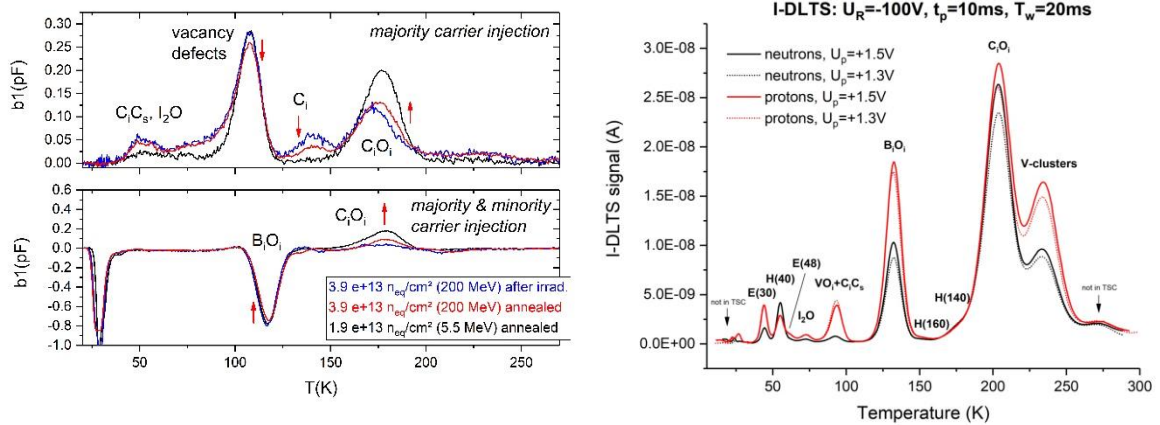


Figure 9 (a) DLTS spectra showing the transformation of carbon related defects during annealing ( $C_i \rightarrow C_iO_i$ ). (b) I-DLTS measurements on neutron and proton irradiated sensors.

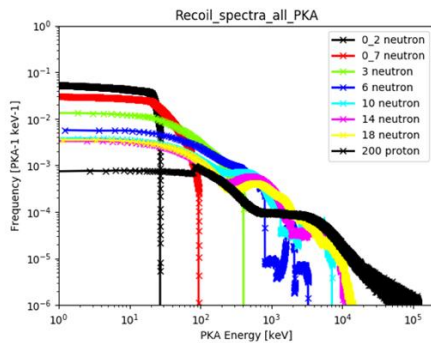


Figure 10. Simulated PKA energy spectra for several neutron energies [MeV] and 200 MeV protons.

**System upgrades:** The cryostat used for the TSC and DLTS measurements in the SSD lab was upgraded with the possibility to use light of four different wavelengths for carrier injection and the range of measurement techniques was extended towards I-DLTS measurements (see example spectrum in Figure 9 (b)). In this technique, current transients are recorded instead of capacitance transients, as used in standard DLTS. The advantage lies in the fact that the technique works on sensors that are fully depleted and in a temperature range below about 30 K, where the majority carriers originating from the shallow doping start to freeze out.

### 2.3. Radiation damage and radiation monitoring techniques

This task is dedicated to the development of radiation monitoring devices and the study of the Non Ionizing Energy Loss (NIEL) concept, which is used to compare and scale the damage impacted on devices in different radiation fields. The goal for the latter is to revise the present NIEL concept for better damage predictions serving both the development of radiation monitoring devices and the predictions of damage occurring in HEP experiments. The work on NIEL started in November 2020 [9] while the development of radiation monitoring devices will begin at a later stage. A particular weakness of the present NIEL concept is, that it does not distinguish the different formation rates of cluster and point defects in the silicon crystal for different particles and particle energies. The effort to revise NIEL is in place, envisioning the production of the new detectors, measuring and evaluating data from already characterized detectors via TSC, CV-IV and DLTS and gaining deeper understanding using simulations, in particular Geant4. From the start of the project, the main work had been carried out on the simulation side. Figure 10 shows 7 different neutron energies and one proton energy of the projectiles being shot at silicon detectors and resulting in the simulated Primary Knocked Atoms (PKA) energy spectra. Continuation of the Geant4 simulation is envisioned to investigate definitions of point and cluster defects, visualize them and compare them with macroscopic and microscopic damage measurements in order to progress towards a revised NIEL concept.

### 2.4. Advanced simulation packages

The complex pixel sensor and readout structures developed within the silicon work packages require advanced simulation tools for a realistic modelling of the detector performance. In particular, the placement of circuitry inside the sensor in monolithic technologies results in very non-uniform electric fields. Therefore, such sensors need to be optimized and simulated with computing-intensive finite-element TCAD simulations. To understand the impact of these optimizations on the detector performance, large event samples are needed. Monte Carlo tools such as Allpix Squared [10] and Garfield++ [11] are therefore developed within WP 1.4, that use TCAD simulation results as input to high-statistics Monte Carlo simulations. These simulations are highly relevant for all sensor developments within the silicon work packages, as they are used to speed up the development cycle and reduce the costs. The main achievements in 2020 concern TCAD, Allpix Squared and Garfield++ simulations for all 65nm and 180nm TJ sensor developments, including the first 65nm MLR run and the MALTA, CLICTD and FASTpix test chips in TJ 180. Furthermore, the tools have been validated against data from various prototype chips and a series of technical meetings has been setup, used as a discussion platform for monolithic sensor simulations for groups from inside and outside CERN. Example results of a combination of 3D TCAD with Allpix Squared and Garfield++ simulations are presented in Figure 11.

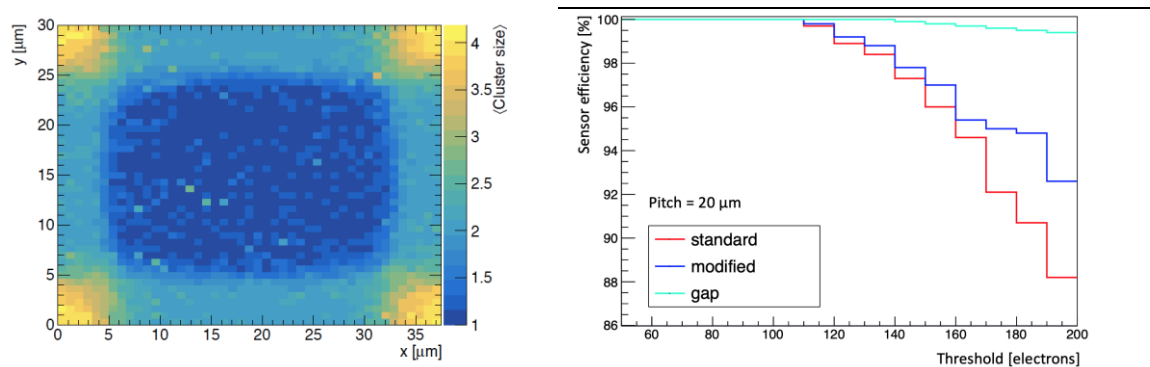


Figure 11: In-pixel cluster size distribution from combined 3D TCAD and Allpix Squared simulations for the CLICTD sensor (left) and sensor efficiency vs. detection threshold from combined 3D TCAD and Garfield++ simulations for different sensor designs optimized for the 65nm TJ MLR run.

### 2.5. Low Gain Avalanche Detectors

In the course of radiation damage studies on LGAD sensors [12, 13] and in close collaboration with WP 1.1. a mechanism of gain suppression was observed and studied. It was found that the measured signal gain in these devices highly depends on the charge density generated by a laser or a charged particle in the device. The electrons generated in the bulk of the devices travel towards the gain layer where the amplification occurs due to the high electric field present in this region. If the charge density arriving at the gain layer region is too high, it will locally reduce the electric field leading to a lower impact ionization factor and in consequence reducing the gain of the device. Several measurements with different detectors were performed showing that ionizing processes that induce higher charge densities in the detector bulk lead to a stronger reduction in the detector's measured gain. One example is given in Figure 12, where the LGAD was illuminated with an IR-laser at different laser intensities. With increasing laser intensity the charge density inside the detector is increasing and therefore the gain is decreasing. In the given example a 50 μm thick LGAD was measured varying the laser intensity from ~ 5 MIPs equivalent up to ~ 30 MIPs.

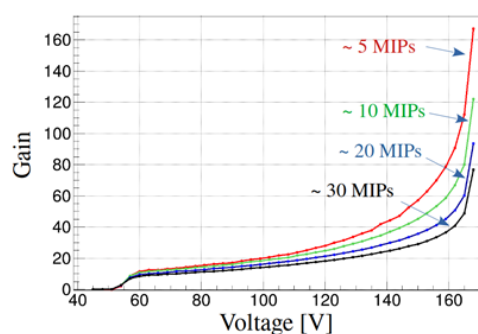


Figure 12 LGAD gain as a function of the reverse bias for different IR-laser intensities.

## 3. Selected publications

- [1] T. Vanat, Caribou – A versatile data acquisition system, PoS TWEPP2019 (2020) 100, <https://doi.org/10.22323/1.370.0100>
- [2] J. Kröger, Silicon Pixel Sensor R&D for the CLIC Tracking Detector, JINST 15 (2020) C08005, <https://doi.org/10.1088/1748-0221/15/08/C08005>
- [3] R. Ballabriga et al., Test-beam characterisation of the CLICTD technology demonstrator - a small collection electrode High-Resistivity CMOS pixel sensor with simultaneous time and energy measurement, CLICdp-Pub-2021-001 (2021), arXiv: <https://arxiv.org/abs/2102.04025/>
- [4] M. Williams, R&D for the CLIC Vertex and Tracking detectors, JINST 15 (2020) 030458, <https://doi.org/10.1088/1748-0221/15/03/C03045>
- [5] M. Wiehe et al., Development of a Tabletop Setup for the Transient Current Technique Using Two Photon Absorption in Silicon Particle Detectors; IEEE TNS, Vol.68, Issue.2, Feb.2021, pages 220-228, <https://doi.org/10.1109/TNS.2020.3044489>
- [6] M. Fernandez Garcia et al. High resolution 3D characterization of silicon detectors using a Two Photon Absorption Transient Current Technique; NIMA 958, 2020 (162865), <https://doi.org/10.1016/j.nima.2019.162865>
- [7] Y. Gurinskaya et al.; Radiation Damage in p-type EPI silicon pad diodes irradiated with protons and neutrons; NIM A 958, 2020 (162221); <https://doi.org/10.1016/j.nima.2019.05.062>
- [8] C. Besleaga et al., Bistability of the BiOI complex and its implications on evaluating the “acceptor removal” process in p-type silicon; Article submitted to NIMA Feb 2021, <https://arxiv.org/abs/2102.06537>
- [9] M. Moll et al., NIEL project - scope – outline, WP1.4. meeting; <https://indico.cern.ch/event/979793/>

- [10] D.Dannheim et al., Combining TCAD and Monte Carlo methods to simulate CMOS pixel sensors with a small collection electrode using the Allpix framework, NIMA964, 2020, 163784, <https://doi.org/10.1016/j.nima.2020.163784>
- [11] Garfield++, <https://garfieldpp.web.cern.ch/garfieldpp/>
- [12] M.Wiehe et.al. Study of the Radiation-Induced Damage Mechanism in Proton Irradiated Low Gain Avalanche Detectors and Its Thermal Annealing Dependence; NIMA, Volume 986, 11 January 2021, 164814, <https://doi.org/10.1016/j.nima.2020.164814>
- [13] E.Currás, Inverse Low Gain Avalanche Detectors (iLGAD) for precise tracking and timing applications, NIMA958, 2020 (162545); <https://doi.org/10.1016/j.nima.2019.162545>

## Contributions to conferences and workshops

- Eric Buschmann, Recent Improvements of the Caribou DAQ System, talk at 9th Beam Telescopes and Test Beams Workshop, 2021, available at: <https://indico.cern.ch/event/945675/contributions/4160095/>.
- Simon Spannagel, What's new on Allpix Squared?, talk at 9th Beam Telescopes and Test Beams Workshop, 2021, available at: <https://indico.cern.ch/event/945675/contributions/4159534/> .
- Esteban Currás, Low Gain Avalanche Detectors for 4-dimensional tracking applications in severe radiation environments, talk at 29th International Workshop on VERTEX detectors, available at <https://indico.cern.ch/event/895924/contributions/3968866/>



## WP2 Gas Detectors

### 1. Introduction

Gas based detectors are a key technology for radiation detection in particle physics experiments. They provide excellent performances for large area, low-mass and radiation hard, relatively cheap and rather easy-to-build detector solutions. Through gas amplification they can intrinsically achieve a large signal-to-noise ratio, releasing requirements in readout electronics and providing excellent single-particle sensitivity. Furthermore they can provide a large dynamic range, stand rates above MHz/cm<sup>2</sup>, achieve space resolution below 100µm as well as sub-ns time resolutions, good energy resolution and cluster counting capabilities.

In the focus of the activities of the WP2 Gas Detectors are large area detection systems, novel technological solutions and a flexible R&D support framework of scientists, tools and infrastructures, capable of supporting new and emerging research activities.

The WP2 activities are embedded in the CERN EP-DT group, in particular in the EP-DT-DD Gas Detector Development (GDD) team and in the EP-DT-FS gas group. In the first year, one fellow, one doctoral student, one technical student and one trainee have been financed by the EP R&D programme. The activities on readout electronics are supported by one doctoral student funded by a special doctoral student programme, the Gentner programme.

All WP2 activities are carried out in strong cooperation with the international RD51 collaboration, the CERN Environmental Protection Steering (CEPS) board and the AIDAInnova international project, creating synergies in the research programme and the use of the available facilities.

The accomplishments of the WP2 start-up phase are reported in the following sections. Ongoing research for precise and fast timing is presented in section 2.1 with a focus on large area and robust PICOSEC Micromegas. The modelling of induced signal in presence of resistive electrodes is described in section 2.2. Section 2.3 highlights the activities focused on DAQ and Front-End (FE) electronics. Section 2.4 presents solutions to mitigate the environmental impact and studies on eco-friendly gases and fluorine based impurities.

### 2. Main activities and achievements in 2020

#### 2.1 Precise timing (25 ps): toward a large area and robust PICOSEC Micromegas

*(F. Brunbauer, M. Lisowska, A. Utrobicic)*

In the PICOSEC Micromegas detector (Fig. 1), incoming particles create Cherenkov photons in a radiator, which are converted into primary photoelectrons by the photocathode. Electrons are pre-amplified in a drift region and amplified by Micromegas. Using this concept, a time resolution of 24 ps for Minimum Ionizing Particles (MIPs) has been measured (NIM A 903 (2018) 317-325). For events distributed across multiple readout pads, about 30 ps time resolution has been measured (NIM A 993 (2021) 165076) opening the possibility to scale up in terms of active area the PICOSEC micromegas concept.

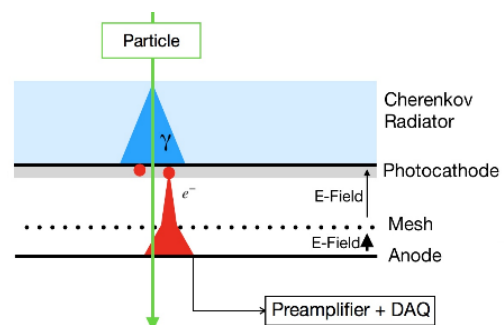


Fig. 1: PICOSEC Micromegas concept [1]



Fig. 2: Top Left: 10cmx10cm micromegas with 100 readout pads. Bottom Left: planarity measurements to monitor and optimize the production processes. Center: prototype under test at the GDD laboratory. Right: Technical drawing of the hermetic prototype.

Within the EP R&D programme, a new tileable prototype with an active area of 100 cm<sup>2</sup> has been built (Fig. 2). Motivated by mechanical simulations, a ceramic-core PCB was chosen and integrated in the EP-DT Micro Pattern Technology workshop to meet pre-amplification gap planarity requirements (<10µm over 100cm<sup>2</sup>) for uniform timing response [2-4]. In parallel, a hermetic detector with low outgassing components and electron beam welded seal, which allows optimal tiling with minimized dead areas, is in preparation (Fig. 2, left) with the support of the Mechanical and Materials Engineering (MME) group of the CERN Engineering Department (EN).

Well-known limitations of CsI photocathodes restrict the potential uses of the detector when high radiation levels are foreseen. Alternative materials and protection layers are under investigation to overcome this problem. The ALICE

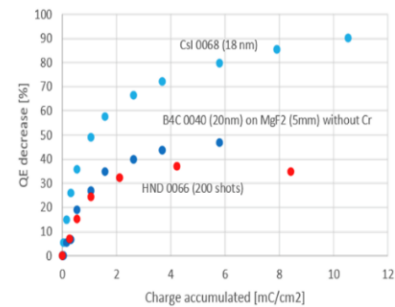
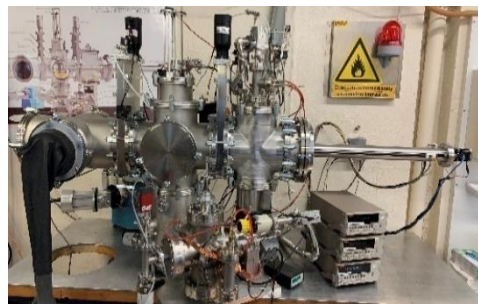


Fig. 3: Left: ASSET facility for QE measurements in transmission and reflective mode and for ion bombardment aging studies. Right: Preliminary ageing measurements [5].

HMPID ASSET (A Small Sample Evaporation & Test facility) setup has been upgraded [5] to allow measurements of absolute Quantum Efficiencies (QE) and ageing. Preliminary measurements on CsI samples and alternative materials as Diamond-Like Carbon (DLC), Boron Carbide (B4C) and Hydrogenated Nano Diamonds (H-ND) have been done (Fig. 3).

Assembly of the hermetic detector and the time resolution measurements at the SPS with the new prototypes and with Carbon based photocathodes will be the next steps. In the future plans, the search of novel photocathodes and protection layers will continue, a resistive multipad micromegas will be designed and built and a readout chains that can be used to readout the full module (100 channels) will be investigated.

## 2.2 Modelling and simulation: Signal induction with resistive electrodes.

(D. Janssens)

Implementing resistive layers in MPGDs has a beneficial impact for large detection system. Space resolution can be preserved with limited number of readout channels. Stability against discharges can be improved for detector based on single amplification stage where simplified production and assembly procedures can be exploited. A simulation framework has been implemented in Garfield++ [6] to model the effect of finite conductivity of resistive elements on the signal. Dynamic weighting potentials are calculated for each specific geometry. These potentials are obtained through analytic



methods for a small subset of detector layouts. For the other cases, numerical methods are used. In our studies, COMSOL provides the time-dependent solutions of the weighting potential, which the Garfield++ can utilise

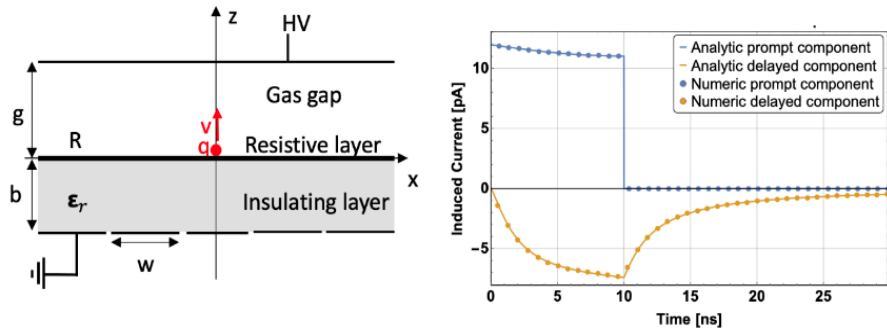


Fig. 4: Left: Schematic representation of the geometry where  $b = g$ ,  $w = 4g$ ,  $\epsilon_r = 3$  and  $R = 0.2 / \epsilon_0 v$ . Right: Induced signal on strip positioned at  $x$ .

to obtain the induced signal. This methodology has been tested on geometries where the exact solution is known (Fig. 4). This activity will have impact on different gas (MPGD, RPC) and silicon based (LGAD) technologies, it will involve several external groups (INFN, CEA/Irfu) and it will strengthen the relevant role played by CERN in detector modelling.

Modelling of different layouts to highlight potential and limitations of the developed framework will be the next step, together with a benchmarking of the simulations via laboratory measurements. In the future plans, the framework will be used to model existing detector (e.g. Micromegas, LGAD) and to design new prototypes (e.g.  $\mu$ RWEL).

### 2.3 Front End Electronics: BNL/ATLAS VMM3a and RD51 SRS

(L. Scharenberg)

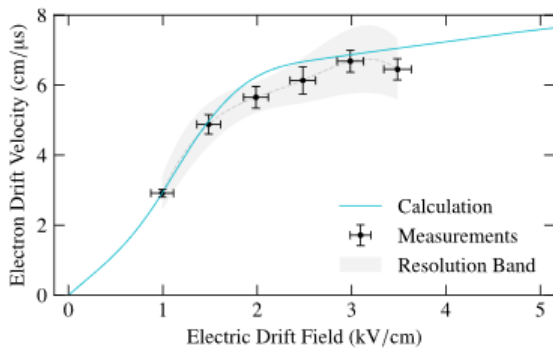


Fig. 5: Electron drift velocity based on Argon fluorescence de-excitation processes measured with SRS/VMM3a

processes in Copper X-Ray absorption from which electron drift velocity (Fig. 5) has been measured [7]. Rate capabilities studies (up to MHz) has been performed in view of future detector test beam campaigns and imaging applications. This activity has been done in the context of a Gentner Doctoral Student program and it will be covered by a task (3.5.2) in the AIDAinnova WP3.

The readout at the SPS of a fully equipped (about 1500 channels) test beam telescope will be the next step. In the future plan, the system will be used to characterize prototypes for future experiments (e.g. COMPASS++/Amber) in laboratory and test beam.

## 2.4 Gas Studies: eco-friendly gases and fluorine based impurities.

(B.Mandelli, M. Corbetta, G. Rigoletti, D. Magatti)

In the context of reducing Green House Gas emissions for particle detectors, several studies are on-going to find suitable alternatives to  $C_2H_2F_4$  (R134a) and  $SF_6$ , mainly used by RPC detectors. A research campaign [10, 11] has been carried on alternatives to  $SF_6$ :  $C_4F_8O$ ,  $CF_3I$ , NOVEC 5510 and NOVEC 4710. Interesting results have been obtained with both NOVEC gases, which have a very low Global Warming Potential (GWP) and very good dielectric properties. In addition, the  $C_4F_8O$  and  $CF_3I$  have been tested: good results have been obtained but both gases do not satisfy all needed requirements (low GWP and no toxicity). In parallel to laboratory tests, long term RPC performance studies with eco-friendly gas mixtures in LHC-like condition are on-going at the GIF++ facility. Next steps will be to carry out studies to better evaluate properties and compatibility of both R134a and  $SF_6$  replacements for RPCs operation at LHC.

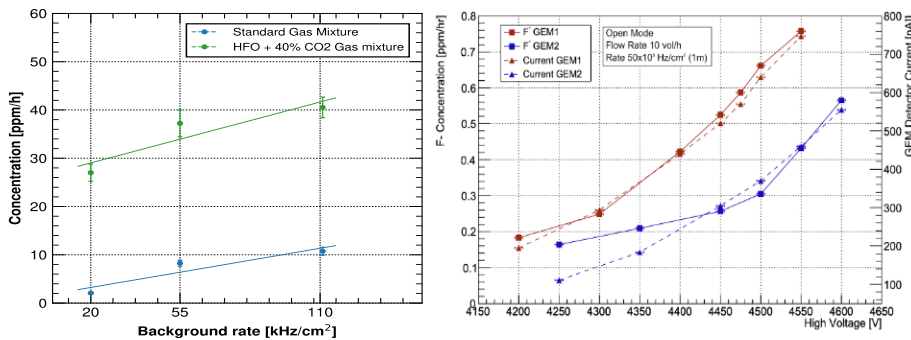


Fig. 6: Left: rate of F- production as a function of gamma rate for the standard and HFO-based gas mixture. Right: Fluoride concentration (left axis) and detector current (right axis) as a function of the high voltage. Both variables increase consistently with the increase of high voltage.

Several gas detectors use fluorinated gases ( $CF_4$ , R134a e HFO) as main gas component or to improve their performance. Under the effects of radiation and electric field, those gases can break into several compounds and free fluoride (F-) ions, which could be harmful for the long-term detector operation. Fluoride production was studied for RPC and Triple-GEMs detectors operated at GIF++ with  $C_2H_2F_4$  (or  $C_3H_2F_4$ ) and  $CF_4$  respectively [12]. For RPC detectors, the impurities production was tested for the standard gas mixture (~95%  $C_2H_2F_4$ ) and the  $C_3H_2F_4$ (HFO)/ $CO_2$  gas mixtures. It was measured that HFO produces about 10 times more fluoride ions than R-134a in equal conditions (Fig. 6, left). A detailed characterization of F- production was realized for triple-GEM detectors operated with  $Ar/CO_2/CF_4$  (45/15/40) gas mixture at different operation conditions. For example, it was found that electric field and irradiation intensity contribute to an increase in the Fluoride ion production (Fig. 6, right).

Next steps will be to continue fluoride measurements for R134a and  $SF_6$  alternatives as well as to prepare measurements on the experiments for the Run 3 operation to better understand the F- production in real conditions at higher luminosity.

## 3 Publications and contributions to conferences and workshops

- [1] F. Brunbauer, "Precise charged particle timing with the PICOSEC detection concept", Instrumentation for Colliding Beam Physics (INSTR-20), February 26, 2020.
- [2] A. Utrobicic, "Update on the planarity of the Picosec Micromegas board", RD51 Collaboration Meeting and the topical workshop on "New Horizons in TPCs", 5-9 October 2020
- [3] A. Utrobicic, Mechanical aspects of CERN GDD 10cm x 10cm new PICOSEC detector, RD51 Collaboration Meeting and Lectures, 22-26 June 2020
- [4] M. Lisowska, "Update on the status of the housing and future sealed housing of the Picosec module", RD51 CM and the topical workshop on "New Horizons in TPCs", 5-9 October 2020
- [5] M. Lisowska, "ASSET-Photocathode characterization device", RD51 Mini-Week and DLC workshop, RD51 MW February 2020

- [6] D. Janssens, "Signals in Resistive MPGDs: an introduction", RD51 Collaboration Meeting and the topical workshop on "New Horizons in TPCs", 5-9 October 2020
- [7] L. Scharenberg, "Improving the position response of MPGDs", RD51 Collaboration Meeting and the topical workshop on "New Horizons in TPCs", 5-9 October 2020
- [8] L. Scharenberg et al., Resolving soft X-ray absorption in energy, space and time in gaseous detectors using the VMM3a ASIC and the SRS, NIM A, Volume 977, 2020, 164310
- [9] L. Scharenberg et al., Gaseous detector studies with the VMM3a ASIC and the Scalable Readout System, 2020 JINST 15 C08026, Instrumentation for Colliding Beam Physics (INSTR2020).
- [10] B. Mandelli, "Performance studies of RPC detectors operated with new environmentally friendly gas mixtures in presence of LHC-like radiation background", ICHEP2020.
- [11] G. Rigoletti, "Performance studies of RPC detectors with new environmentally friendly gas mixtures in presence of LHC-like background radiation", RPC2020.
- [12] M. Corbetta, "Studies on Fluorine-based impurities production in Triple-GEMs operated with CF4-based Gas Mixture", IEEE2020.

# WP3 Calorimetry

## WP3.1 Noble Liquid Calorimetry

### 1. Introduction

The next generation of calorimeters for collider experiments will have to feature at the same time high granularity, very good energy resolution and a strong control over the systematic uncertainties and acceptance. Noble Liquid Calorimetry is a very promising candidate to meet these requirements and the challenges that have to be overcome seem within reach for an application at the time-scale of the next generation of collider experiments. As described in the next sections, this work package contains R&D to overcome these challenges, it is organized around the two following main activities: the design of a new type of readout electrode realized as multi-layer PCBs and the development of new high-density feedthroughs.

Currently two fellows are working for this WP3.1: one entirely funded by the EP R&D program; the second fellow shared equally between EP R&D and funds from CERN Cryo Lab. Several external groups have joined the effort with students, postdocs, staff physicists and engineers contributing: IJCLab (F), Prague Charles University (CZ), University of Copenhagen (DK) and University of Edinburgh (UK). Bi-weekly meetings have started mid-2020 to follow-up on the progress, usually O(15) people are connected each time (<https://indico.cern.ch/event/1014834/>). Additional resources have been requested by AIDAInnova and a preliminary allocation of 80k€ was obtained.

### 2. Main activities and achievements in 2020

#### 2.1 Read-out electrode design optimization

Noble-liquid calorimetry is being used in ATLAS. In order to fulfil the requirements of the next generation of collider experiments the read-out granularity needs to be increased. This can be realized by the use of multi-layer read-out electrodes extracting the signal via long transmission lines while keeping the cross-talk at an acceptable value. Thanks to multi-layer PCBs, these transmission lines can run inside the readout electrodes and take the shortest path towards the calorimeter boundaries. Cross talk between calorimeter cells can be mitigated by the addition of ground shields around the signal traces (as shown in the picture), however such ground shields will also increase the cell capacitance which translates linearly into an increase of signal noise.

A precise estimation of the cross-talk, signal attenuation and noise has to be carried out in order to evaluate the feasibility of such a design and to optimize the various free parameters. To this end, a detailed description of one readout PCB cell has been implemented into a finite-element software (COMSOL®) and first results of cell capacitance and transmission line impedance have been extracted, validating the assumptions made for the FCC-hh detector proposal.

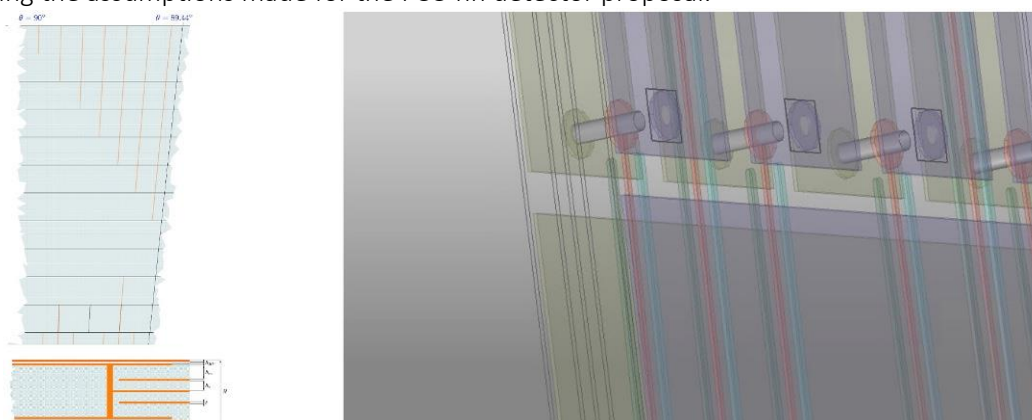


Figure 1: Left: Layout of the readout electrode multi-layer PCB showing the transmission lines seen from the top and from the side. Right: Cadence® model of part of the PCB (zoom on vias of the second longitudinal compartment).

Following the recent update of the European Strategy for Particle Physics, the FCC-hh calorimeter concept has been modified to fit an FCC-ee detector proposal (larger inner radius, shortened depth, ...). The longitudinal granularity has also been increased from 8 layers (in the FCC-hh proposal) to 12 layers. A full tower of this new PCB design, shown in the left top picture of Figure 1, has been implemented in a manufacture-oriented software (Cadence®) in collaboration with the CERN PCB Design Office. This model is being ported to the finite-element software simulations and will serve as a first step towards the prototyping phase.

The new FCC-ee calorimeter design has been implemented in the FCC-SW Full Sim framework and performance studies/optimization have started. In parallel, the transition of the calorimeter implementation and reconstruction to the Key4hep framework has been initiated, in close collaboration with the CERN EP-SFT group.

## 2.2 High-density signal feedthroughs

The higher read-out granularity of future noble-liquid calorimeters leads to a strong increase in the number of read-out channels and, consequently, to the need for high-density signal feedthroughs that ensure the passage of the signals from the cold calorimeter to the warm electronics outside.

In order to achieve a density between 20 and 50 wires/cm<sup>2</sup>, the use of connectors on each side of the flange should be avoided. R&D on a new, high-density feedthrough flange has started. The geometry of the flange is presented in Figure 2 and it consists of a stainless-steel grid with 3D-printed structures with slits, allowing the cables to pass through. These slits will be then filled with a glue ensuring the leak-tightness of the flange.

To select the best glue candidates, short stainless-steel tubes have been filled with 8 different glues and resins, they have been thermally shocked in liquid nitrogen (77 K) and leak tested. Furthermore, pieces of 4 different 3D-printed or fiberglass materials (Accura25, Accura48, MY750 and G10) have been designed, fabricated in collaboration with the Polymer Laboratory at CERN, and thermally shocked in liquid nitrogen. In this way, it was possible to verify the eventual appearance of cracks in the materials and to determine the coefficients of thermal expansion at low temperatures. After selecting the best epoxy and glue candidates, the final samples have been fabricated. In these samples, the future strip cables are represented by strips made of polyimide passing through the 3D-printed epoxy pieces and the glue.

To simulate the extreme conditions in the calorimeter, an experimental setup has been constructed to perform pressure and leak tests on the final samples at 80 K and at ambient temperature. Moreover, a numerical simulation has been performed in ANSYS Fluent, to analyze the temperature and pressure evolution in case of a vacuum break accident in the experimental setup.

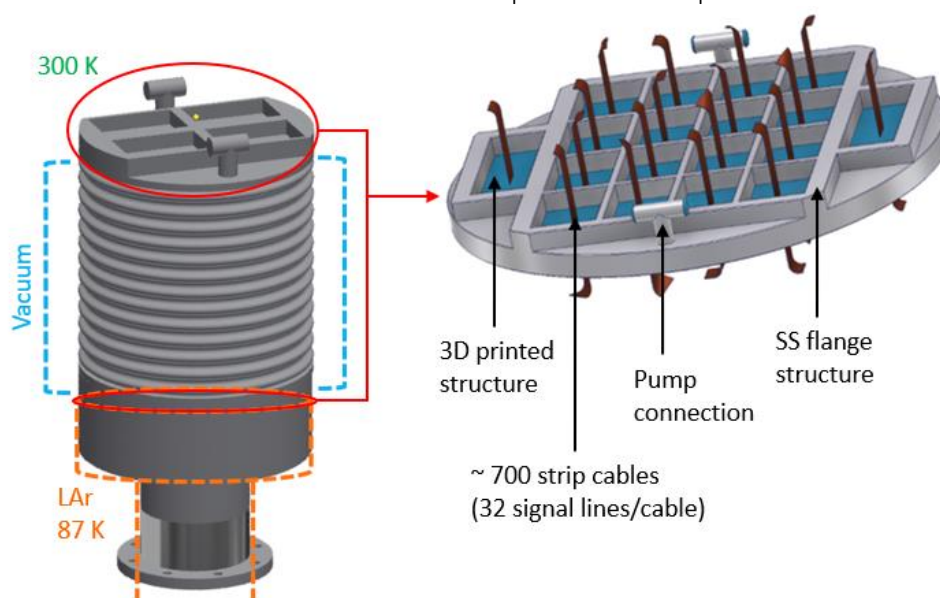


Figure 2: Schematic illustration of a feedthrough and conceptual design of a high-density feedthrough flange.

## 2.3 Publications and contributions to conferences and workshops

Two talks at the 4th FCC Physics and Experiments Workshop (<https://indico.cern.ch/event/932973>):

- Talk 'R&D on Noble Liquid Calorimetry for FCC'  
<https://indico.cern.ch/event/932973/contributions/4062113/>
- Talk 'R&D on light-weight cryostats and on high-density FTs'  
<https://indico.cern.ch/event/932973/contributions/4062114/>

Frequent presentations at bi-weekly 'Noble Liquid Calorimetry Meetings'

## WP3.2 & WP3.2.1: R&D on SPACAL Calorimeter and Prospective R&D for Scintillator Based Calorimeters

(Summary prepared by L. Martinazolli, M. Pizzichemi, M. Salomoni, E. Auffray, P. Roloff, A. Schopper)

### 1. Introduction

The objective of the SPACAL R&D is to develop a "spaghetti" type, sampling calorimeter for the upgrade of the current LHCb electromagnetic calorimeter. Performance requirements are a spatial resolution of order millimeters, an energy resolution of 10% sampling term and close to 1% constant term, a time resolution of the order of 20 ps at 100 GeV, radiation hardness up to 1 MGy for the innermost part of the calorimeter and 200 kGy for the region surrounding the innermost modules. Several active materials and geometries were investigated by means of experimental test benches and Monte Carlo simulations. Among the crystals studied in WP3.4, garnet crystals are the best candidates for a SPACAL, thanks to their cutting-edge radiation hardness and attractive timing properties. Scintillating and timing properties of other scintillators such as scintillating DSB glasses have been investigated. One fellow, Matteo Salomoni, joined the group in August 2020 and a Ph.D. student, Roberto Calà, joined in November 2020. The core resources provided by the EP-RD program for 2020 were one Fellow for WP3.2 and one Technical Student for WP3.4, which were extended by students from other funding sources at CERN. We collaborated with several partners from LHCb and the Crystal Clear collaboration (Barcelona University, Bologna University & INFN, MISiS Moscow, IHEP Protvino, Giessen University, FZU Prague, RINP in Minsk).

### 2. Main activities and achievements in 2020

#### 2.1 R&D on garnet materials

A GAGG fibre was irradiated with protons of 24 GeV at the CERN IRRAD facilities up to 1MGy. We observed a decrease in attenuation length from 100 cm to 34 cm, compatible with the experiment requirements based on simulations (Sec. 2.2). Several 2x2x3 mm<sup>3</sup> GAGG samples from various producers worldwide were characterized to explore and understand the current scintillation performance of the material. Light output was measured using <sup>137</sup>Cs gamma sources, whilst scintillation emission time profiles were measured with a <sup>22</sup>Na gamma sources. The light output ranged between 27900 and 49500 photons/MeV and the fastest samples showed scintillation time components below 70 ps rise time and 50 ns decay time. The time resolution (FWHM) was evaluated with 511 keV photons emitted by <sup>22</sup>Na gamma sources and employing fast silicon photomultipliers (SiPMs), obtaining a best value of 77 +/- 2 ps full width at half maximum. These results (see table 1) marked a significant step forward with respect to the past state of the art of the material. GAGG emerges as a mature solution for scintillation-based particle detectors in the harsh environments of the High-Luminosity phase of the LHC, as well as neutron detection, and gamma ray spectroscopy. Following these results, GAGG from different producers were selected to equip cells of the SPACAL prototype discussed in Sec. 2.3, along with more standard material such as YAG.

Table 1: Scintillation properties and timing performance of the most promising GAGG samples of this campaign. Light output is known +/- 3%, decay time +/- 4 ns, Time Resolution +/- 2 ps.

Sample	Photons [MeV <sup>-1</sup> ]	Output	Effective Decay time [ns]	Time Resolution at 511 keV (FWHM) [ps]
C&A GFAG	32 140		56	77
Crytur	29 310		67	87
ILM	27 900		56	82
Epic Fast	30 330		57	77
Fomos*	37 700		86	91
Sichuan Tianle	38 580		74	85

\*GAGG employed so far.

## 2.2 SPACAL Calorimeter simulation

A full Monte Carlo simulation framework has been developed, with the capability to study energy and timing resolution performance of individual SPACAL modules, as well as the full SPACAL part of the LHCb ECAL. Energy resolution performance was found to be  $9.1\% \oplus 1.4\%$  (sampling term  $\oplus$  constant term), while timing resolution is expected to be better than 50 ps above 5 GeV and around 10 ps at 100 GeV, using the current standard LHCb calorimeter PMTs (R7899-20). The MC framework has been also used to estimate the deterioration in performance of SPACAL modules due to radiation damage. The results suggest that a module based on W and GAGG, with longitudinal segmentation, would retain good performance (constant term of energy resolution better than 2%) even after 1 MGy of irradiation. The MC has been validated for various prototypes using test beam measurements, as summarized in the next section

## 2.3 Test beam @ DESY

Test beam data of a SPACAL-W configuration were acquired with electron beam energies ranging from 1 to 5 GeV. The module consisted of 3x3 cells of  $1.5 \times 1.5 \times 14 \text{ cm}^3$  with front-to-back separation at 4 cm ( $7X_0$ ). The 9 cells were equipped with different crystals: YAG, GFAG, FOMOS, and ILM. Figure 3 shows a picture of the test beam setup.



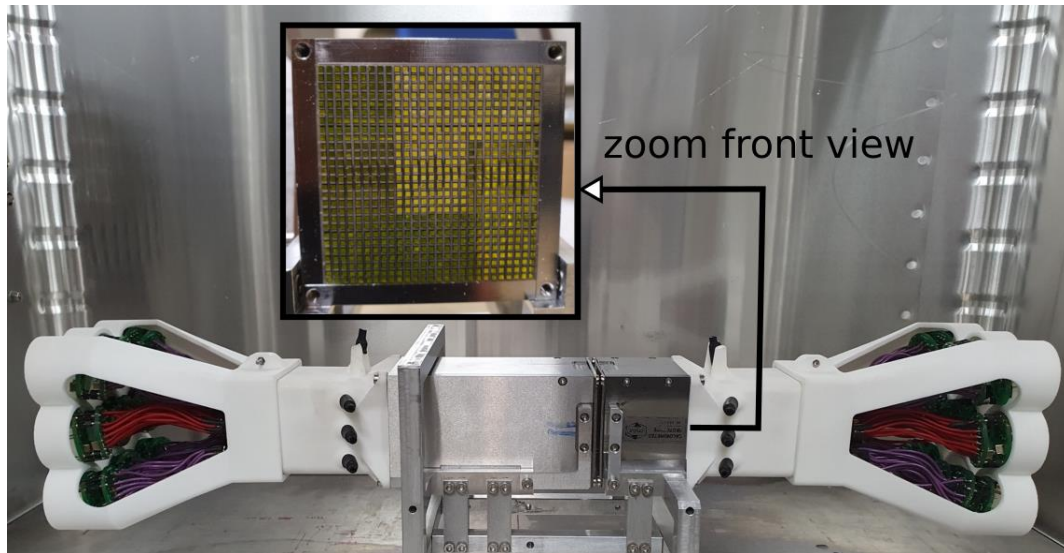


Figure 3: Test beam configuration with front and back sections read out separately. The zoom insert shows a detail of the 9 cells equipped with different scintillating fibers (with readout removed).

Energy resolution of this prototype has been measured using R7899-20 PMTs and compared with simulations, as shown in Figure 4. A timing resolution of 34 ps was obtained with GFAG scintillating fibres at 5 GeV, in good agreement with MC simulation, averaging front and back contributions and using R7600 MCD-PMT readout with DRS4 electronics. The selection of such a PMT is the result of an ongoing hardware investigation for timing and light collection optimization. Figure 5 shows a summary of the timing results obtained for the different materials at different energies.

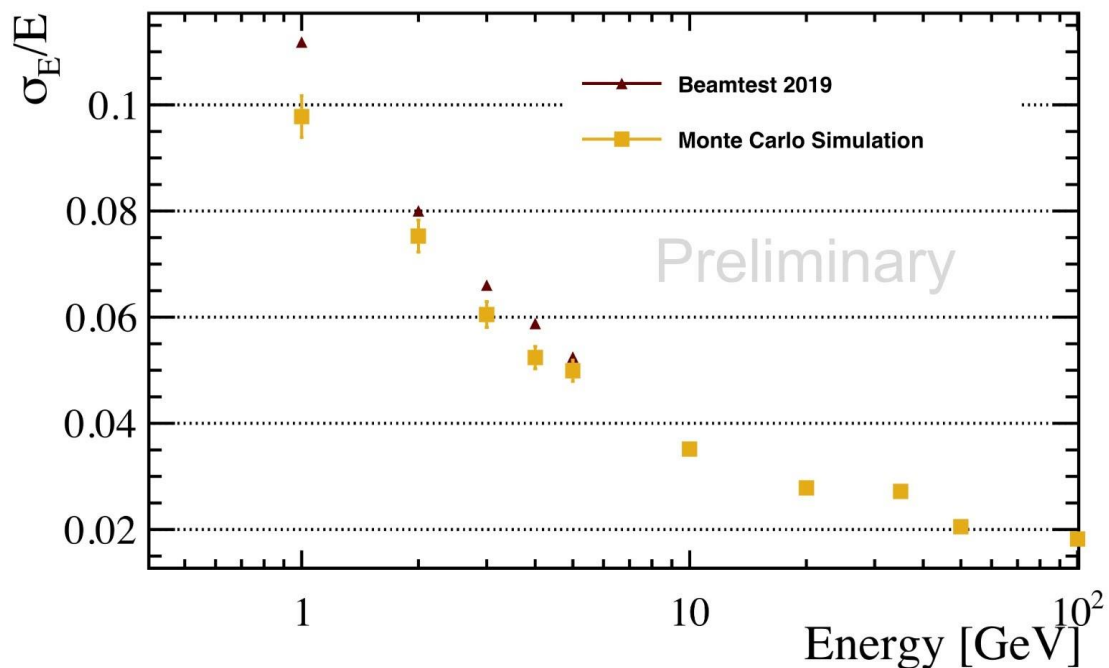


Figure 4: Energy resolution as a function of energy comparing test beam data (up to 5 GeV) and simulation (up to 100 GeV).



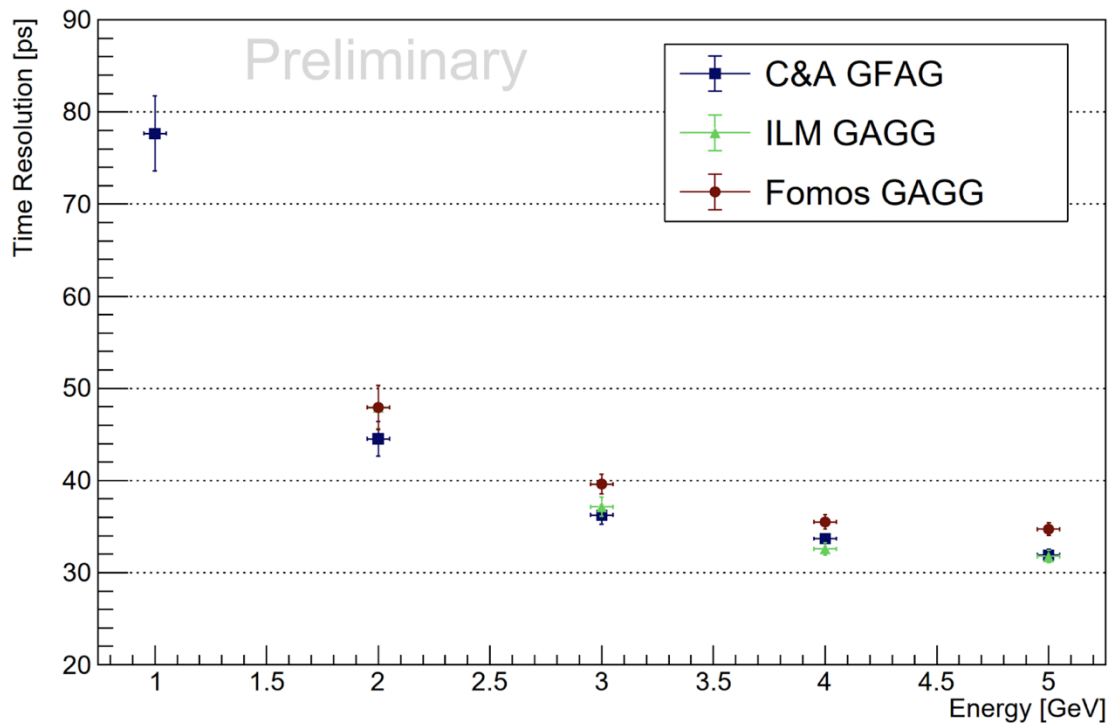


Figure 5: Measured time resolution up to 5 GeV for the different materials under study.

## 2.4 Publications and contributions to conferences and workshops

### Publications

- L. Martinazzoli, "Crystal Fibers for the LHCb Calorimeter Upgrade," in IEEE Transactions on Nuclear Science, vol. 67, no. 6, pp. 1003-1008, June 2020
- M, Pizzichemi, "The Phase II upgrade of the LHCb calorimeter system", in Journal of Instrumentation 15 (05), C05062, 2020
- L. Martinazzoli, N. Kratochwil, S. Gundacker, E. Auffray, "Scintillation Properties and Timing Performance of State-of-the-art  $Gd_2Al_2Ga_3O_{12}$ ," accepted for publication in NIM A

### Presentations

- L. Martinazzoli on behalf of the LHCb & Crystal Clear SPACAL R&D group, "ECAL Testbeam Results and Simulations", 4th Workshop on LHCb Upgrade II, 9<sup>th</sup> April 2019, Amsterdam, Netherlands
- L. Martinazzoli on behalf of the LHCb & Crystal Clear SPACAL R&D group, "Crystal Fibres for LHCb Calorimeter Upgrade", SCINT 2019 conference, 30<sup>th</sup> September 2019, Sendai, Japan
- L. Martinazzoli on behalf of the LHCb & Crystal Clear SPACAL R&D group, "Crystal Based Calorimeter R&D", EP-R&D Session, October 2019
- M, Pizzichemi on behalf of the LHCb & Crystal Clear SPACAL R&D group, "The Phase II upgrade of the LHCb calorimeter system", CHEF2019, 25 November 2019, Fukuoka, Japan
- M. Pizzichemi on behalf of the LHCb & Crystal Clear SPACAL R&D group, "ECAL Technologies", 5th Workshop on LHCb upgrade II - 30 Mar - 1 Apr 2020, Barcelona
- Ph. Roloff on behalf of the SPACAL R&D and Simulation/Reconstruction for the ECAL Upgrade 2 groups, "Upgrade 2: ECAL studies", 97th LHCb week, September 2020
- L. Martinazzoli, N. Kratochwil, S. Gundacker, E. Auffray, "Scintillation Characterisation and State-of-the-art Timing Performance of  $Gd_2Al_2Ga_3O_{12}$  Single Crystals", IEEE NSS MIC 2020 conference online
- M. Salomoni on behalf of the SPACAL R&D group, "Test-Beam Desy 2020: results", LHCb week, Dec 2020

## Posters

- L. Martinazzoli on behalf of the LHCb & Crystal Clear SPACAL R&D group, "*Development of a Sampling Module for the LHCb Electromagnetic Calorimeter Upgrade*", IEEE NSS MIC 2020 conference online

WP3.3: R&D for Si based calorimetry (Postponed)

WP3.4: R&D on RICH detectors (activity starts in 2021)

WP3.5: R&D on plastic scintillating fibre trackers

A novel concept for higher light yield scintillating fibres which potentially would also be more radiation tolerant than the current generation has been investigated with Geant4 simulations. The concept includes having more than one wavelength shifter in the same part of the fibre. This was previously not supported in Geant4 and therefore needed to be changed in the framework. This change has been made and is now available to all Geant4 users. The simulation of the new fibre concept is almost completed and depending on the results, it might be decided to move forward and produce a test fibre based on the new concept.

## WP4 Mechanics

### 1. Introduction

In 2020, a program was launched to develop lightweight solutions for the next generation HEP experiments with a focus on mechanical supports and thermal management of future vertex tracking detectors and on next-generation ultralight cryostats for Detector Magnets and LAr Calorimeters. Following an initial review phase to identify the key requirements, in the first half of the year, the Working Group is now investigating possible design solutions and new materials.

In WP4, the engineering effort on the design of the mechanics for future trackers is driven one side by near-future applications, like the possible ALICE ITS3 upgrade for RUN4, and on the other side it is exploring futuristic solutions for long-term developments. The design of a trackers' mechanical structures is inherently linked to the cooling solutions, and, while gas-cooling studies for lepton colliders have already started, a detailed investigation on new coolants to achieve low temperatures in hadron colliders will be launched in the second half of 2021. This development line on tracker mechanics and cooling is perfectly aligned with the AIDA-Innova new program with which resources and industry support will be synchronized and - if possible - shared.

The R&D to reduce further the material and the wall thickness of cryostats by using carbon fibre reinforced plastics, has started from the studies of the present ATLAS LAr/SC-Magnet cryostat, made of aluminium. The advantages and implications of a full carbon composite design, which accounts for the more stringent requirements of future colliders, are being evaluated by the Working Group (5cm minimum wall thickness for LAr calorimeter, and 40 cm for Detector Superconductive magnet thickness, including cryostat). Prototypes, to validate leak tightness across the wall of a carbon composite cryostat, and carbon flanges sealed interfaces, have been produced and are currently under test.

In parallel to the developments on ultralight mechanics, the Working Group as a second development line has started a detailed analysis to identify the needs of future detectors for automated and robotic solutions for their inspection, opening, access, and maintenance as facing the record-levels of radiation expected in future colliders. State-of-the-art robotic solutions suitable for HEP Experiments, and best detector design practice from a robotic-friendly perspective, have been investigated and summarized in guideline documents. Concrete immediate needs have been identified in the current LHC detectors, through a close exchange with the Experiments Technical Coordinators, and some robotic solutions that could be applied for the remote inspection of the current detectors are being investigated.

The Working Group relies on young and motivated students and fellows<sup>1</sup>, who despite the adverse period, have enthusiastically worked at the different development lines. While the center-of-gravity of the group is in EP-DT, several links have been created with other Working Groups and Laboratories<sup>2</sup> inside CERN and with Institutes and Companies outside<sup>3</sup>.

<sup>1</sup> Tracker: Massimo Angeletti, Desiree Hellenschmidt, Matheo Dias; Gabriele Fiorenza; Cryotank: Soledad Molina; Robotics: Lorenzo Teofili)

<sup>2</sup> WP1, WP3, WP8, TE-CRG-CI, TE-VSC-BVO, EP-DT-DSF, EP-DT-DD, EN MME)

<sup>3</sup> Robotics: San Jorge Tecnologicas, ANYbotics, Boston Dynamics, KUKA, Petoj; Low Mass Structure: Alphacam, XJet, Fraunhofer IKTS, Sarris, ERG Aerospace, Entegris, Allcomp, American Elements, Discoeurope; CTD, Solvay, Australia's Global University)

## 2. Main activities and achievements in 2020

### 2.1. Low Mass Structure

#### 2.1.1. Tracker mechanics and cooling

To minimize the material in the acceptance of future trackers, a key question is whether it is at all possible to build a detector that would completely abstain from using an electrical substrate and an active cooling circuit. One possibility could be the approach followed by the ALICE Collaboration, to design and construct a novel vertex detector consisting of curved wafer-scale ultra-thin silicon sensors (down to 50-30  $\mu\text{m}$ ) arranged in perfectly cylindrical layers, featuring an unprecedented low material budget of 0.05 % X 0 per layer. One single bent sensor covers an entire half-cylindrical layer. The Working Group, in collaboration with colleagues from ALICE, is working on the development of the mechanics and cooling system of such a detector, the ALICE ITS3. The mechanical conceptual design of the ITS3 is based on an external carbon shell, used as an exoskeleton, and ultra-light carbon foam supports that keep the layers bent in position and act as cooling radiators. The heat dissipated by the sensors is removed by convection through a forced airflow between the layers. In this first year, the Working Group has developed a procedure and a tool to bend the large silicon chip and has supported the validation of the wire bonding process on a curved sensor for the connection to the power/data FPC (Fig1). The group has characterized different carbon foams and has set up a wind tunnel to validate the first full-scale engineering model for both thermal and stability performance.

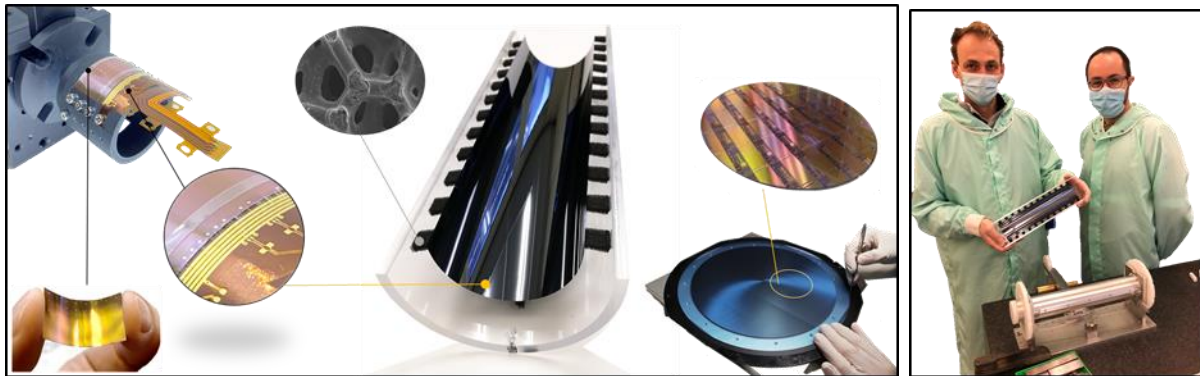


*Fig.1 Large silicon chip, based on stitching technology, bended to form half-cylinder, and glued in position with carbon foam wedges that act as mechanical support and thermal radiator; small scale curved chip wire bonded to Flex Printed Circuit.*

In addition to the minimum material budget requirements, the possibility to put the first layers closer to the IP represents another central requirement for future generation vertex detectors. In view of a possible ALICE upgrade for LHC Run 5, the Working Group has started working on a futuristic concept of a retractable vertex detector inserted inside the beampipe, shielded in a secondary vacuum, that, after the beam injection, can contract and place the first detection layer at few millimetres from the interaction point. In addition to the development of a first design and the identification of a number of suitable engineering solutions, the Working Group has started a collaboration with the CERN Vacuum Group and with the CERN Central Workshop to assess design choices and manufacturing feasibility.

The search for the limits, towards which cooling solutions can be further developed, is complemented in the Workpackage by studies for liquid active cooling for higher radiative environments. Here solutions which allow to replace titanium or steel pipes by plastic pipes, e.g. Kapton or of sacrificial materials to create vascular networks in carbon composite structures are under investigations. The technology originally developed for the ALICE ITS, which employs ultra-thin Kapton pipes to flow water below atmospheric pressure, is currently under study by the Working Group for high pressure applications involving two-phase CO<sub>2</sub> (Fig2, left picture). At the same time, standard Silicon

microchannel solutions used for CO<sub>2</sub> at high pressure are under study. Their application in vertex or tracker detectors in future HEP experiments are challenged by their typical bulky and complicated interconnection as well by their fragility. The idea to have modular microchannel substrates (M $\mu$ CS) that can be assembled and interconnected like LEGO bricks has been developed (Fig 2 , middle picture).



*Fig.2 Different on detector microcooling solutions under development and test (left to right, CO<sub>2</sub> test set-up for thin plastic pipes, 3d printed microchannel LEGO, study for microvascular network embedded in a carbon coldplate)*

A plug-n-play in-plane hydraulic interconnection, that automatically engages between two adjacent modules, mechanically locked through the LEGO feature, has been tested, so far, up to 40 bars. Additive manufacturing (AM) technologies, based on plastic (acrylic and epoxy-based photosensitive resins) and ceramics (Zirconia, Alumina, Silicon carbide, and Aluminium nitride) have been considered as an alternative to the present silicon etching process. Based on this concept, several interconnection configurations have been designed, analysed and tested in the Working Group. The baseline configuration is so-called LEGO [1]; design variations (Clip-based, Spring-based, Rails-based) have been then developed and breadboard models have been considered for tests and comparison [2]. Hybrid designs between Si and AM microchannel cooling substrates are also considered for M $\mu$ CS and being investigated to grasp, from each technology, the upsides minimizing the downsides. This concept opens the way to the use of microchannels also for the coverage of the large surface with silicon pixel chip sensors, providing the possibility of easy mechanical and hydraulic connectivity and re-workability.

### 2.1.2. Ultra-light Cryostat

Is it possible to build cryostats for future detectors with lighter and thinner walls to reduce the impact of the material budget on physics performances? To answer this question, the Working Group has started to study in detail the present ATLAS cryostat, collecting all the available information and reconstructing step by step its layout and assembly sequence. A close collaboration with the groups of WP3 and WP8 has allowed to benefit from the experience of colleagues who worked in the construction of the original cryostat, as well as to determine the new requirements for future ones [3]. In this process, two main challenges have been identified: cryostat leak tightness in carbon composite solutions and reliable sealed joints included in the cryostat design, either for assembly or for services feedthrough.

A preliminary analysis has been performed to assess the advantages of different light design choices that range from full carbon, aluminium sandwich, and carbon sandwich. The initial focus has been on the identification of the best suitable carbon material and layout that would fulfil the challenging requirements on leak tightness at cryo-temperatures. Full carbon cryotanks with no metallic liner, are being studied as well in aerospace programs (CCTD project driven by NASA, CHATT European program) for Liquid Oxygen (LOx) and Liquid Hydrogen (LH<sub>2</sub>) storage for future launchers. After a state-of-the-art review [4], the Working Group has contacted several companies and academic institutions investigating this field, e.g. CTD, Solvay and Australia's Global University among others. To enhance the resistance to microcracking damage and its propagation at cryogenic temperatures, a high strain



composite material with toughened resin has been identified, CTD-133/IM7. An optimal layup of this material, based on the use of ultrathin (70 gsm) plies interleaved in between thicker plies (140 gsm), is being investigated, in order to allow higher cross-ply density and a significant reduction of the void content in the laminate. A cylindrical demonstrator pipe ( $D_i=100\text{mm}$ ) has been designed and built for manufacturing verification and characterisation. While, in aerospace, cryotanks are mostly based on spherical or ellipsoidal monolithic design, in HEP the need to insert a detector inside the cryostat, and the large number of feedthroughs for services, introduce a new key requirement that is the sealing of cryostat joints. This completely unexplored feature is under investigation. Based on CERN's experience in UHV sealed joints for standard aluminium flanges, and on limited know-how in specific carbon composite applications, a preliminary design has been developed and two carbon composite flanges with a spring-energised metal Helicoflex seal have been manufactured and are now ready to be tested.



*Fig.3 Pipe and flanges with special carbon materials and layup for leaktightness verification at cryogenic temperatures*

In all the prototyping work, an out of autoclave approach for the final curing process has driven our resin system choice. The goal is to characterize demonstrator scaled models the production process of which could be applied to large cryostats, where dimensions will be prohibitive for curing in autoclave.

A test campaign to characterise these initial design choices will be carried out in close collaboration with CERN Cryolab & Instrumentation section, with the support and expertise of our WP3 colleagues. The two demonstrator units, i.e. the thin wall carbon shell and the carbon sealed flanges assembly, will be brought to working conditions (77K, 5bar) and a helium leak test will be performed to assess the leak tightness (Fig3).

## 2.2. Robotics

The main activity for the first year was to identify available automated/robotic solutions, compatible with the needs of future HEP detectors. Two documents, [5] and [6], have been compiled listing possible solutions. The former is a literature review of the state-of-art of robotic systems. It focuses on robotic hardware and shows the robots that could be used in a detector environment. The second document is a guideline to build detector components that are optimized to be manipulated by robots. It focuses on the service interfaces and it shows design examples of automatic and robotic friendly components used in different fields (as the JET and ITER Tokamak experiments, the International Space Station, the CERN accelerator complex and the ISOLDE experiment at CERN).

The studies have confirmed the need for two main systems: a system to open large-mass detectors for access (the so-called Motion Of Volumetric-massive Equipment System or, in short, MOVES) and, a system to manipulate the detector components and to perform surveys (the so-called HANDling and Survey ON detector or, in short, HANDS-ON). Furthermore, there is the need for a standard interface for service connection that can be manipulated by a robotic arm. This interface should include a mechanism for automatic matching and alignment of the service connector plug and socket (Mechanism for AuTomatic service Connection Handling, or, in short MATCH).

Some problems linked to the use of robots in current and future detectors have been identified. The Technical Coordinators of the experiments which have been visited (ALICE, CMS, and LHCb) agree that a robotic system capable of inspecting the detector cavern at the time at which the accelerator is running would be highly beneficial. However, a major problem for a robotic system in an environment as the detector cavern with the running accelerator is the strong magnetic field. Indeed, most of the autonomous robotic devices are actuated by electric servomotors that may not behave as expected with a strong background magnetic field. Since the applications of robotics in high magnetic fields environment are limited to high-energy physics experiments and aluminium foundry, probably, the robotic industry will not tackle this problem in the near future. Thus, in the context of this R&D, experiments on the response of different kinds of electric motors to an intense magnetic field have been started. Furthermore, alternatives to the electric motors are being explored, piezoelectric motors and compressed air motors (San Jorge Technological, a company that develops compressed air drones, have been contacted for a preliminary conceptual study).



*Fig.4 ANYmal\_C moving in CERN Experiments' similar environment, visit at ANYbotics*

Also, some robotic solutions that could be applied for the survey of the current detectors have been found on the market. Quadruped robots, as SPOT from Boston Dynamics and ANYMAL C from ANYbotics, are considered good candidates to move in a difficult environment as a detector cavern, provided that they survive the magnetic field. Both the companies have been contacted and a visit to the Zurich side of ANYbotics has been performed (Fig.4).

To further explore the capability of the quadruped robots, some low-cost items (PETOI Bittle) have been bought for prototyping. These low-cost robots will be tested under magnetic fields (up to 0.5 T) and will be used to perform simple tasks in a controlled environment.

### 3. Publications and contributions to conferences and workshops

- [1] LEGO-based interconnections for modular microfluidic cooling substrates (M $\mu$ CS) for future silicon tracking detectors in High Energy Physics (HEP). Being submitted
- [2] Hook-based interconnections for modular microchannel cooling substrates (M $\mu$ CS) for future silicon tracking detectors in High Energy Physics (HEP). Being submitted
- [3] Report on requirements for Future Detector Superconductive Magnet Liquid argon calorimeters. To be published in EDMS
- [4] State of the art for Carbon Composite Cryotanks. To be published in EDMS
- [5] State of the Art of Robotic Solutions in Harsh Environment. To be published in EDMS
- [6] Best Practices for the Design of High Energy Physics Detectors to be Operated by Robotic and Automated Systems. To be published in EDMS

# WP5 IC Technologies

## 1. Introduction

Microelectronics is widely recognised as one of the key enabling technologies for present day and future High Energy Physics experiments. At present most ASIC developments for the LHC upgrades are based on the 65nm node (with 130nm being used in less demanding applications). One of the aims of Work Package 5 is to provide the HEP community with a solid infrastructure in state-of-the art CMOS technologies for the design of complex mixed-mode ASICs for future applications. Another component of the work package is to develop novel approaches for DCDC conversion allowing efficient transfer of power to the components in the heart of the detectors.

At present Work Package 5 has 2 active components. There are 2 Fellows and 2 students currently employed on the WP.

## 2. Main activities and achievements in 2020

### 2.1. IC Technologies (WP 5.1)

One of the first tasks of this part of the work package was to choose the technology to be supported in the coming years. Four CMOS processes were considered: two 28 nm bulk technologies, 22 nm FDSOI, 16 nm FinFET. Radiation hardness measurements of two 28 nm bulk CMOS processes are promising (up to 1 Grad). A reference to the full report is indicated below. The criteria used to choose the supported technology were as follows: radiation tolerance, accessibility, technical support, availability of IP blocks, expected long-term availability, cost. The technology chosen is the 28 nm TSMC HPC+ process which is available to our community via IMEC. There are MPWs 12 times per year and a minimum chip size of 1 mm<sup>2</sup>. It should be noted that the radiation measurements have to be reconfirmed for this technology as the flavour now available (HPC+) differs slightly from that previously tested (HPC).

Looking beyond 28 nm, systematic TID testing of 16 nm FinFETs is foreseen. Some radiation testing of the 22FDSOI process from GF confirmed the expected poor radiation behaviour for TIDs above ~1Mrad. A versatile standardized testbench for SEU and TID evaluation of sample silicon chips manufactured on different processes has been designed by the Fellow employed by the WP.

A Common Design Platform for the HPC+ process is under development and a common metal stack chosen (1P9M\_5X1Z1U + UTRDL). A preliminary subset of transistor flavours to be supported has been identified but not yet fully confirmed. The Incremental Technology Database approach has been adopted enabling updates to the Process Design Kit to be achieved with much less effort than previously. There are numerous digital libraries available for the technology and a subset is being studied.

Ideas for a radiation tolerant System on Chip ecosystem are being developed. Standardized design methodology will be supported and fully verified building blocks made available to the community. Some applications may benefit from standardized programmable blocks (e.g. RISC-V processor)

We are still seeking the extension of the MTUA (Master Technology User Agreement) with TSMC which covers 65 nm and 130 nm nodes to 28nm and permits design sharing between participating institutes. Negotiations have been slow as our community has little weight in the foundry business.

In order to facilitate the flow of information between members of the community a 28 nm Forum has been established. Members of the community were invited to subscribe to an e-group which gives password protected access to the meetings and presentations. Two meetings have been held each with over 100 participants and the feedback from the ASIC design community has been very positive.

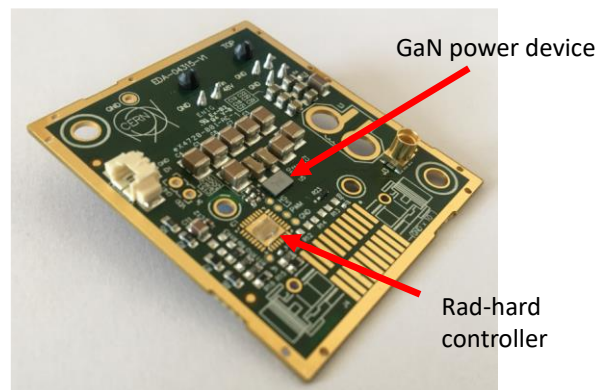
### 2.2. Power distribution (WP 5.2b)

In the WP5.2 the advancements have been remarkable. Several prototypes of DCDC converter have been successfully designed and tested. A non-rad-hard version of a converter able to provide 12 V output from 48 V input with a Gallium Nitride (GaN) power stage and a commercial controller was designed. The efficiency is very high reaching 94% with a load of 10 A. In the meanwhile, radiation tests (Single Event Effect, SEE and Total Ionizing Dose, TID) on the GaN chipset have been carried out

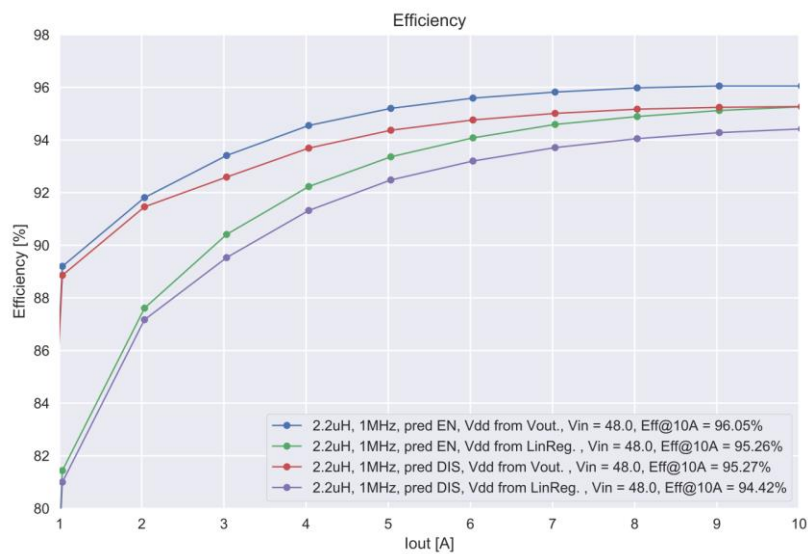
showing very good intrinsic radiation tolerance of these devices, that can be easily used for most CERN experiment applications.

A rad-hard controller was designed in commercial High Voltage 0.35  $\mu\text{m}$  technology, able to provide the right timing to the GaN power MOSFET and reducing their diode conduction with a circuit called predictive dead time. An internal linear regulator can provide from a maximum voltage of 80 V the 12 V needed by the GaN chipset.

This rad-hard controller was integrated in a buck converter (from 48 V to 12 V) with GaN power stage, whose resulting board is shown in the following picture.



The Efficiency of this converter is higher than the previous one thanks to the predictive logic and the possibility to feed the GaN chipset from the  $V_{\text{out}}$  at 12 V. 96% can be reached at 10A output.



This converter has been successfully irradiated with X-rays up to a TID of 60 Mrad without any change in the output voltage or efficiency. Displacement damage tests and Single event tests are scheduled in the next months.

### 3. Publications and contributions to conferences and workshops

---

- [1] Giulio Borghello, “Ionizing Radiation Effects On 28 nm CMOS Technology” [https://espace.cern.ch/asics-support/Shared%20Documents/2020\\_Report\\_TID\\_effects\\_28nm.pdf](https://espace.cern.ch/asics-support/Shared%20Documents/2020_Report_TID_effects_28nm.pdf)
- [2] 1<sup>st</sup> 28nm Forum <https://indico.cern.ch/event/970389/>
- [3] 2<sup>nd</sup> 28nm Forum <https://indico.cern.ch/event/1009040/>
- [4] Giacomo Ripamonti, “On-detector power: current technologies & ongoing R&D”, LHCb upgrade 1b/2 electronics kick-off workshop, Nov. 2020 <https://indico.cern.ch/event/960837/>
- [5] Pablo Antoszczuk "48V-12V DC-DC GaN Converters: development and first results, ESE-ME Topical meeting Jan 2021 <https://indico.cern.ch/event/996633/>



## WP6 High Speed Links

### 1. Introduction

The evolution of pixel, tracker, and timing detectors clearly points to the need of developing high-bandwidth detector-embedded data communication systems that will operate in increasing hostile radiation environments. The “High Speed Links” work package (WP6) addresses these topics by aiming at the development and demonstration of radiation tolerant components such as custom ASICs and Optoelectronics devices. The system-level aspects are also investigated by the use of state of the art FPGAs in an effort to keep compatibility with commercial developments and to set up an environment where the concepts and components being developed can be validated. 2020 saw the FPGA and Optoelectronics activities started with the ASICs activity to start in 2021 (with the hiring of a PhD student and Fellow).

Providing laboratory infrastructure to support the testing and evaluation of data transmission links operating at high data rates (28 Gbps NRZ and 28 GBd PAM-4) was the target fully achieved for the FPGA activity. Early experimentation with commercially-available equipment and components allowed to probe in which directions the communications industry is moving. A key question is how can HEP systems be made to be compliant with industry standards and to what extent they can deviate from those? In the physical layer, no clear standard has emerged proving that the field is not yet mature and that the WP6 developments will need to remain open to future evolutions.

The optoelectronics activity was dominated by the successful demonstration of a full-custom silicon Photonics Integrated Circuit (PIC) that contains several variations of the optoelectronics elements needed to build on-detector radiation hard optical links. In particular, this allowed the demonstration of a ring modulator-based transmitter operating at 10 Gbps, a key component towards the implementation of a Silicon Photonics (SiPh) system. Modelling of devices and radiation effects on optoelectronics components is also of key importance. Commercially-available SiPh CAD tools were explored to model the transfer function of the custom ring modulator as a first step to subsequently include the radiation effects on the design process of the SiPh components for HEP. Radiation testing also took place during 2020 with the tests done on the ring modulator revealing the device to be robust to TID doses close to 5 MGy.

A PhD student, Milana Lalovic, and fellow, Chaowaroj Wanotayaroj, joined the optoelectronics and FPGA activities (starting on the 2<sup>nd</sup> of March and the 1<sup>st</sup> of June respectively). Despite the Covid-19 restrictions, the participation of the ESE staff in the EP R&D programme allowed for a relatively early start and the year was productive.

### 2. Main activities and achievements in 2020

#### FPGA-1: FPGA-based system testing and emulation

Successful implementation of high-speed links in HEP environments has, in general, relied on tracking the communications industry developments and, where possible, on the use of Commercial Off-The-Shelf (COTS) components. For LHC, this has been possible for the counting room electronics but full-custom components were needed for the on-detector system. Success thus required the latter to adhere, as much as possible, to industry standards for interoperability. FPGA vendors currently target their products at data centres aiming for the highest bandwidths possible for a given semiconductor technology node (current high-end FPGAs feature 9 Tbps aggregated bandwidth). It is thus imperative for WP6 to track these developments and a good fraction of 2020 was dedicated to acquiring the instrumentation needed (a 28 GHz bandwidth sampling scope was purchased) and high data rate optoelectronics so that laboratory systems could be set up. Besides the actual hardware, studies were

also made to understand what impact the emerging data transmission protocols and modulation schemes will have on future HEP systems.

#### *PAM-4 standard analysis*

The current drive to high data transmission bandwidths pushes the manufacturers to depart from the standard ON-OFF Keying electrical and optical modulation schemes (e.g., NRZ) and, instead, to adopt multilevel modulation schemes in an attempt to cram higher data rates into the same electrical/optical bandwidths. These higher order modulation schemes trade-off signal-to-noise ratio for bandwidth. The industry is currently moving to Pulse Amplitude Modulation with 4 levels (PAM-4) for both electrical and optical transmission. Analysis of these standards revealed that PAM-4 standards are still in development and that many sub-standards are currently proposed by the industry, targeting line rates from 50 Gbps up to 400 Gbps (still in evolution), distances from 100 m to more than 10 km and using various multiplexing techniques and fibre types. New key figures of merit were identified to characterize complex PAM-4 eye diagrams (electrical PAM-4 and NRZ eye diagrams acquired using the N1092C high-end sampling oscilloscope are shown on Figure 1 left and right respectively) and it was understood that Forward Error Correction coding is indispensable to achieve error free data transmission (even in the absence of single-event upsets typically present in the HEP systems).

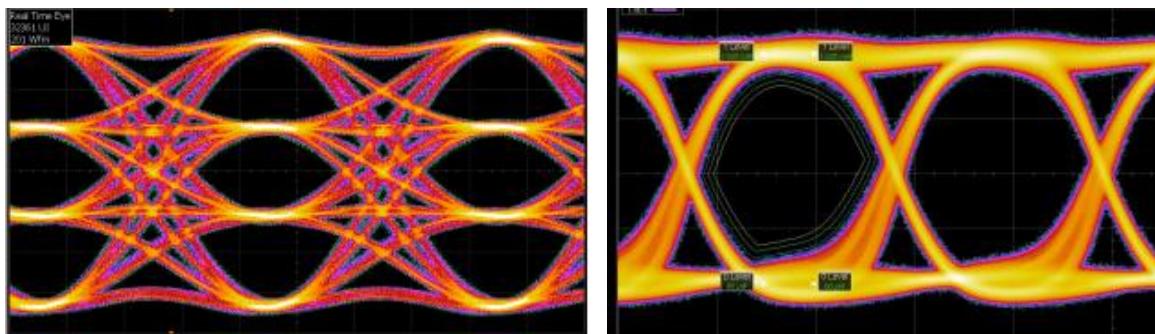


Figure 1: (left) PAM-4 modulated optical signal at 28 GBd (56 Gbps). (right) NRZ modulated traditional optical signal featuring 28 Gbps.

#### *Selection of FPGA-based hardware and optoelectronics devices:*

A selection of FPGAs, optical devices, passive equipment, and high-end instrumentation was made in order to implement and assess 28 Gbps and 56 Gbps NRZ and PAM-4 links over electrical and optical media. The large variety of standard references of optoelectronic devices, on one hand, and the very limited number of available modules on the market, on the other hand, highlighted the lack of maturity of the market. The market is still dominated by proprietary solutions (requiring the use of transmitters and receivers from the same company with patented encoding scheme) competing to be standardized, without a specific common standard arising yet.

#### *Implementation and first measurements on the Physical Layer*

On the Electrical front, a full simulation model was implemented in the electrical domain as a reference for future tests. It allowed as well to estimate potential coding gains on the electrical links and predict the impact of various hardware or environmental parameters. The first tests and characterization performed on 28 Gbps NRZ and 56 Gbps PAM-4 electrical streams confirmed the simulation results and allowed fine tuning of embedded FPGA parameters in order to improve the signal integrity (Figure 2, left). On the optical front, similar analysis highlighted the noisy nature of this physical layer on currently available COTS (Figure 2, right) and emphasized the need of a strong Forward Error

Correction scheme to reach a target error rate of  $10^{-9}$  or below (the expected error rates without FEC are around  $10^{-4}$ ).

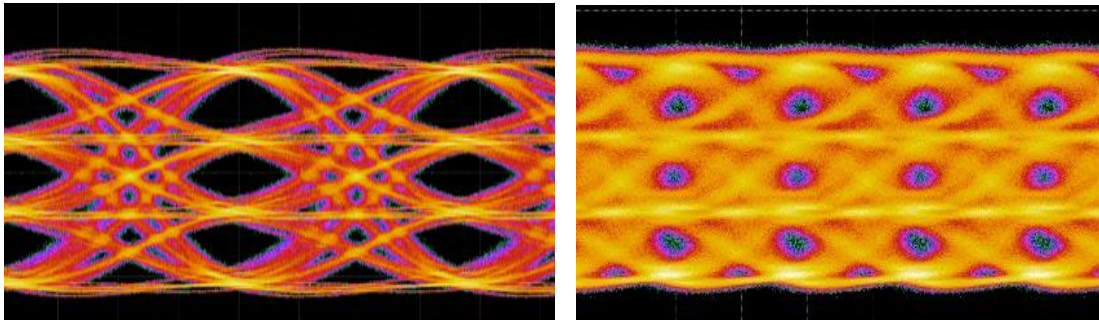


Figure 2: (left) Electrical PAM-4 Eye obtained with a high frequency Sampling Oscilloscope on the electrical output of a Virtex Ultrascale evaluation board. (right) Optical PAM-4 eye obtained with the same oscilloscope on the optical output of a PAM-4 transceiver connected to the same evaluation board.

#### First experience with the Data Layer implementation

On the firmware front, it has been shown that IP cores provided by FPGA vendors are not yet fully functional. This required the implementation of custom logic to perform Bit Error Rate analysis and slowed down the progress on the firmware side.

#### OPTO-1: Silicon Photonics System & Chip Design

A new test chip (PICv2) based on the IMEC Silicon Photonics process was received from the foundry in 2020. The test chip builds upon previous experience to include several new structures including ring modulators and Wavelength Division Multiplexing systems based on such modulators, as well as Mach-Zehnder modulators and Germanium photodiodes similar to those tested previously.

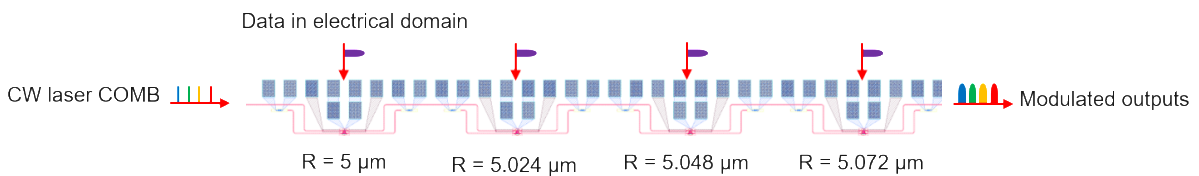


Figure 3: Four-wavelength Transmitter structure based on Ring Modulators

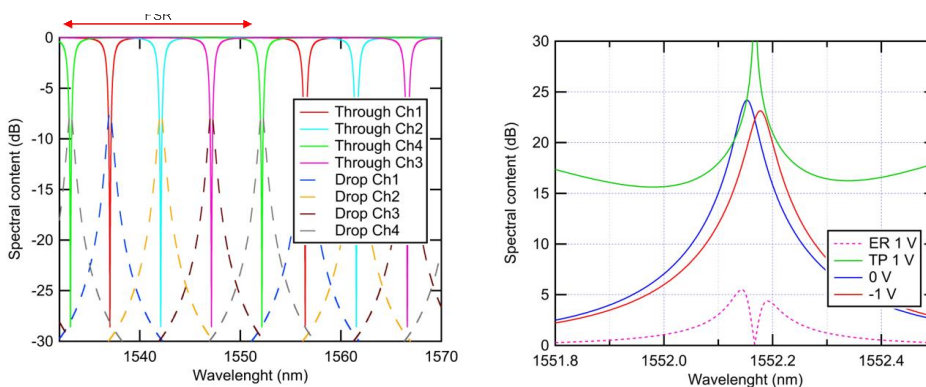


Figure 4: (left) spectral response simulation of the 4-ch WDM Transmitter shown above; (right) simulated Ring Modulator transmission performance with 1V modulation

The layout of a four-wavelength Transmitter structure based on ring modulators is shown in Figure 3, and the simulated performance in Figure 4. From the simulated performance we see that a relatively

small modulation voltage of 1 V, which is within reach of the 28 nm CMOS process targeted by the chip design task of WP6, provides reasonable performance.

The fabricated chip was mounted onto a test PCB and pigtailed with optical fibres at CERN using a high-precision manual pick and place machine that is able to achieve the alignment tolerance of the order of 1  $\mu\text{m}$  required to achieve proper optical coupling. Figure 5 shows the assembled PICv2. PICv2 also contains a number of new features that allow us to characterise many of the system aspects of a full silicon photonics transmission system, for example micro-heaters to tune the operating wavelength, and polarisation diversity structures to help couple light into the Photonic Integrated Circuit (PIC).

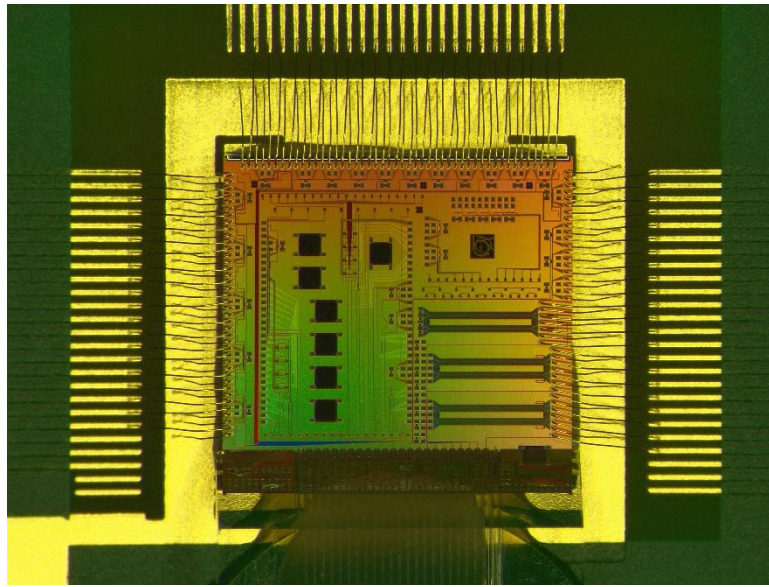


Figure 5: Micrograph of the fabricated PICv2 wire-bonded onto a test board and pigtailed with a 24-channel single-mode fibre array. The optical pigtail is at the lower edge of the picture the chip size is 5 x 5 mm<sup>2</sup>.

The system concept moving forwards is to target the use of Ring Modulators for future Silicon Photonics systems. Such devices offer many advantages, including small size, lower driving voltage and high efficiency. On the other hand, these very small devices (ring diameter <math><10 \mu\text{m}</math>) are quite sensitive to temperature, both external and self-heating due to the optical power absorbed by the structure.

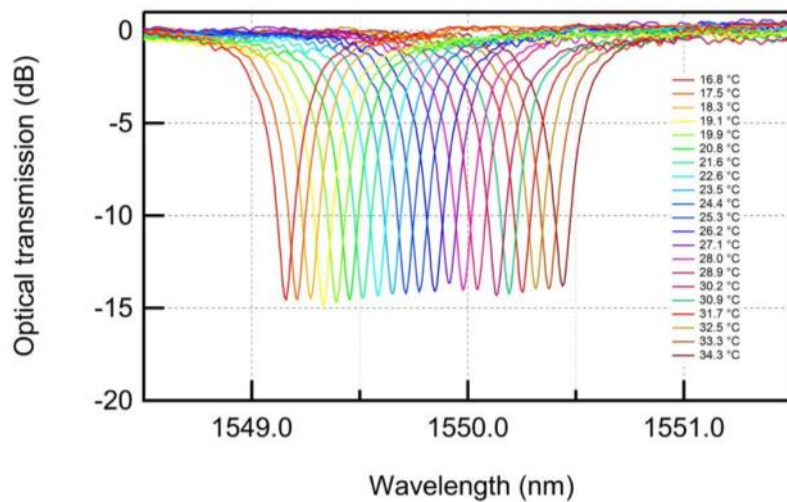


Figure 6: Optical transmission as a function of wavelength, showing the ring modulator temperature-controlled wavelength tuning possible using micro-heaters fabricated on the new PICv2.



For this reason, micro-heaters are included in PICv2 and Figure 6 shows the tuning the resonance wavelength over a large enough wavelength range in order to be able to lock the operating wavelength to a fixed wavelength grid. Having obtained this result paves the way for implementing a wavelength locking and stabilization system in future that could eventually be implemented in the system ASIC that will operate a Silicon Photonics link.

Demonstrating high-speed operation of the ring modulators requires the availability of suitable instrumentation. In this first year of the project we have been limited to existing instrumentation that works up to 12.5 Gbps, which was used to show that it is possible to drive ring modulators at such data-rates. An example eye diagram is shown in Figure 7. Effort has been put into selecting and evaluating test equipment that is able to both generate the appropriate driving signals and visualise the output eye diagrams for both NRZ and PAM4 modulated signals up to 28 GBd. This instrumentation will be available in the near future to continue the device and system characterisation at the target data rates.

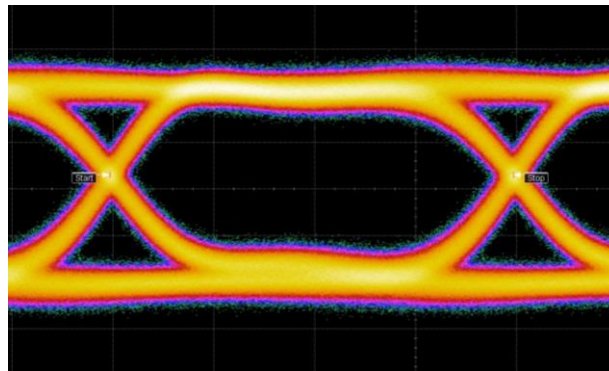


Figure 7: Measured optical eye diagram (12.5 Gbps) of one of the ring modulators integrated onto PICv2.

## OPTO-2: Silicon Photonics Radiation Hardness

The first irradiation test of the new PICv2 was carried out using the X-ray generator facility within EP-ESE, during which PICv2 was irradiated up to a total dose of almost 5 MGy. The test protocol was developed based on our previous experience with the first Silicon Photonics PIC, in particular with respect to the bias levels applied during the irradiations. The first tests showed that the process improvements made by IMEC have also been beneficial to the radiation tolerance of the modulators. The results shown in Figure 8 compare the change in modulation efficiency of ring modulators across process generations, with the new generation being significantly more radiation tolerant than the previous one. This is very encouraging as it will minimize the amount of customisation that will be necessary in order to service the needs of early adopters of this technology, where ultimate radiation tolerance might not be the most important constraint.

During this first radiation test we were also able, for the first time, to vary the operating temperature of the devices using the micro-heaters built into the design. This adds an additional degree of freedom to the irradiation testing, as we can now closely control the device operating at an elevated temperature. Eventually, in a full system, these heaters will be set in order to tune the operating wavelength. We are thus adapting the test protocol to check the impact of local heating on the radiation response. Early results from this first study do not provide clear conclusions yet because the effect is convoluted with the variation in design parameters, and further study of the parameter space will be carried out in the near future.



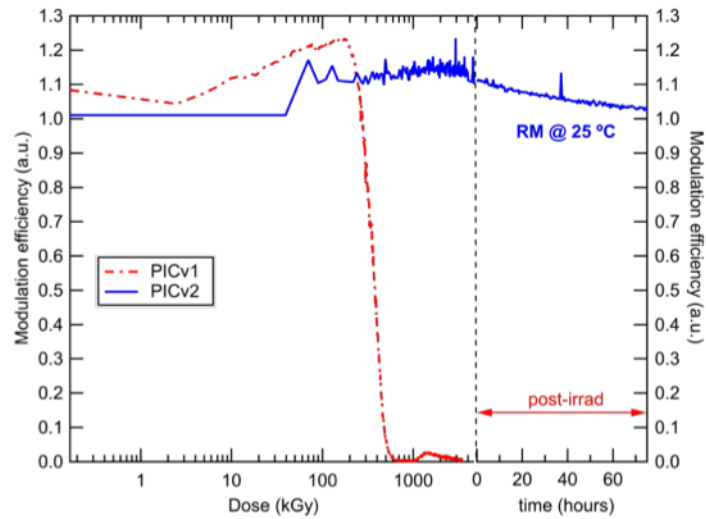


Figure 8: Modulation efficiency as a function of dose, showing the clear improvement in the radiation tolerance of the latest generation Ring Modulator on PICv2 vs. the previous generation on PICv1.

### 3. Publications and contributions to conferences and workshops

---

Presentation “Silicon photonics for rad-hard high-speed links”, C. Scarcella, CMS Inner Tracker Future Technologies Workshop, 13 November 2020

## WP7 Software

### 1. Introduction

Software plays a critical role in modern HEP experiments, with the efficient handling of event data being key to physics success. In the Software Work Package, we focus on areas where increases in efficiency and improvements in performance will enable future experiments to maximise their physics return and reduce the overall time-to-results of physicists doing analysis. The R&D WP consists of tasks which will speed-up accurate *simulation*, optimise event *reconstruction* in modern detectors, improve *analysis* throughput and deliver well tested and coherent *software stacks* to experiments. All this is centred in the new hardware landscape of *heterogeneous computing*.

The Software WP made an excellent start in 2020, meeting the challenges of team building and personnel integration during the Covid pandemic. Fellows and students were recruited in a timely fashion and all tasks were able to make a start, with the exception of the Faster Simulation task which began only this year. Hardware purchases were held-up but were finalised with the help of CERN IT procurement. CERN IT also agreed, exceptionally, to host our R&D machines in the data centre.

Our Turnkey Software Stack work has been well integrated with other participants via the HEP Software Foundation, with the participation of DESY and IHEP. The Analysis work is in synergy with the ROOT team's plans and the reconstruction projects work hand in hand with CMS (calorimetry) and ACTS (tracking). There will be new synergy this year with the AIDAInnova EU funded project.

### 2. Main activities and achievements in 2020

#### 2.1 Turnkey Software Stack

EP R&D supported Valentin Volkl as a fellow since January 2020, working on Key4hep – the turnkey software stack. This task will provide future collider projects with a common software stack allowing optimal choices for simulation, reconstruction and analysis studies as well as detector optimisation studies. In the first year the efforts have been to merge different tools from the CLIC and FCC detector studies. The Key4hep stack will support, as applicable, multiple interchangeable options for a given tool, e.g., different fast simulation tools or different calorimeter reconstruction tools. The most important ingredients for this development are an event processing framework, an event data model, a geometry system, as well as tools to compile, deploy, and set up the stack.

The Gaudi framework, which was already in use for FCC, and is also used by the LHCb and ATLAS experiments, was chosen as the basis for the Key4hep project. Generic parts of the FCC software were transferred into the Key4hep framework core (k4FWCore) package.

For both the CLIC and FCC software DD4hep was already the detector description system.

For the event data model a new package – EDM4hep – was developed based on PODIO<sup>3</sup>, a generic data model generator, used for the original FCC EDM. The event data described by EDM4hep is very similar to the LCIO event data model as used for the CLIC detector studies. Figure 1 shows the relationship of the event data classes. As a first use case of Key4hep, before the full simulation and reconstruction is available, an output module for the Delphes fast simulation package was created, which already allows users to familiarize themselves with the EDM4hep event data model and interfaces.

To adapt the algorithms from the iLCSoft frame in use by CLIC to Gaudi a *wrapper* around the existing algorithms was developed, which will allow almost seamless integration of these algorithms into the

---

<sup>3</sup> Gaede, F. and Hegner, B. and Mato, P. PODIO: An Event-Data-Model Toolkit for High Energy Physics Experiments, J. Phys. Conf. Ser. 898 2017. DOI: [10.1088/1742-6596/898/7/072039](https://doi.org/10.1088/1742-6596/898/7/072039).

Key4hep framework and continues validation of the ongoing efforts. In the long term this wrapper will be replaced by proper algorithm ports. The similarity between EDM4hep and LCIO also eases adapting the existing algorithms.

For the compilation of the individual packages of the software stack the Spack package manager<sup>4</sup> was chosen, after being reviewed positively by the HSF Packaging Group<sup>5</sup>. Together with a deployment on CVMFS releases and nightly builds are provisioned for all users of the Key4hep software stack.

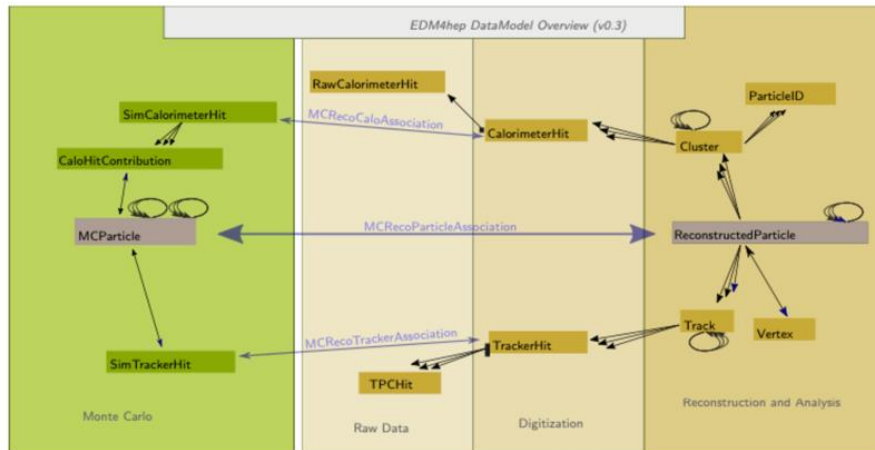


Figure 1. EDM4hep data model class relationships. *Raw data* hits can be linked with *digitized objects* and then to *reconstructed clusters*, tracks, particles and vertexes. These can all be associated with the original artefacts produced by the *Monte Carlo* simulation.

## 2.2 Reconstruction – Calorimetry

The development of novel algorithms for calorimeter reconstruction at high pile-up is taking advantage of the new High-Granularity calorimeter (HGCal) proposed for the forward region for the CMS Phase-2 upgrade and, more generally, from CMS experience with Particle Flow (PF) techniques.

The R&D activity is developing a new software framework, TICL (The Iterative CLustering) that is fully modular and will be re-usable in other (future) experiments using high-granularity calorimeters and facing high density environments. The EP R&D has supported Erica Brondolin in this task since summer 2020. New techniques and algorithms spanning several fields – from clustering to machine learning, graph theory, and modern computer architectures – will be investigated, also taking into account information from the surrounding detectors, as is normal in PF. All modules are designed as swappable plugins within the CMSSW framework, with heterogeneous architectures and portability in mind. Finally, TICL is mostly geometry independent, which makes it a great candidate for shower reconstruction in high-granularity calorimeters.

TICL processes hits that are built in the detector and returns particle properties and probabilities. The building blocks used by TICL are the 2-dimensional *LayerClusters* that are built by the CLUE algorithm<sup>6</sup>. These 2D objects are grouped iteratively into 3-dimensional clusters, so-called *tracksters*, which should

<sup>4</sup> Todd Gamblin, Matthew P. LeGendre, Michael R. Collette, Gregory L. Lee, Adam Moody, Bronis R. de Supinski, and W. Scott Futral. [The Spack Package Manager: Bringing Order to HPC Software Chaos](#). In *Supercomputing 2015 (SC'15)*, Austin, Texas, November 15-20 2015. LLNL-CONF-669890.

<sup>5</sup> L. Sexton-Kennedy, B. Hegner, & B. Viren. (2016, March 23). HSF Packaging Working Group Report. HSF-TN-2016-03. Zenodo. <https://doi.org/10.5281/zenodo.1472340>.

<sup>6</sup> M. Rovere, Z. Chen, A. Di Pilato, F. Pantaleo, and C. Seez. [CLUE: A Fast Parallel Clustering Algorithm for High Granularity Calorimeters in High-Energy Physics](#). *Frontiers in Big Data* 3, 2020.

correspond to different showers. Each iteration inside TICL is composed of different steps. The starting point of each iteration is to define a seed region, which can be a small region around a reconstructed track or can span the entire HGAL acceptance. The Cellular Automaton algorithm is then run for the pattern recognition task and the defined selection criteria applied to final tracksters. Before starting the next iteration, all 2D LayerClusters belonging to the tracksters are masked to reduce the combinatorics.

In 2020 TICL was made more resilient when tested on simulations including up to 200 pile-up, improving single particle and EM shower reconstruction. In particular:

- Iterations were re-ordered and a new specific iteration for track seeded electromagnetic (EM) showers was introduced.
- Trackster reconstruction was improved in favour of high energy objects.
- A Particle-ID interpretation as been included with the aim of promoting each trackster to the corresponding particle candidate.

Finally, work has begun to extend the TICL concepts to future experiments and allow it to be flexibly deployed outside CMSSW, as an extension, as stand-alone or integrated into a common stack, such as Key4hep.

### 2.3 Reconstruction - Tracking

The EP R&D tracking initiative works within the larger ACTS project, which includes R&D lines in machine learning and parallelisation and acceleration strategies. Successful R&D projects are integrated into the ACTS core software package for deployment and distribution.

The EP R&D effort has supported Moritz Kiehn from March 2020. He has coordinated the integration of the ONNX machine learning inference library into the code and has helped with the integration of an auto-differentiation library. To develop efficient parallel processing in tracking (Figure 2) it is essential that the data model allow for efficient data processing and the redesign of the ACTS data model was led by EP R&D, where the measurement EDM was drastically simplified. This critical task allowed the release of the first quasi-stable version of ACTS that can advertise its API version to clients.

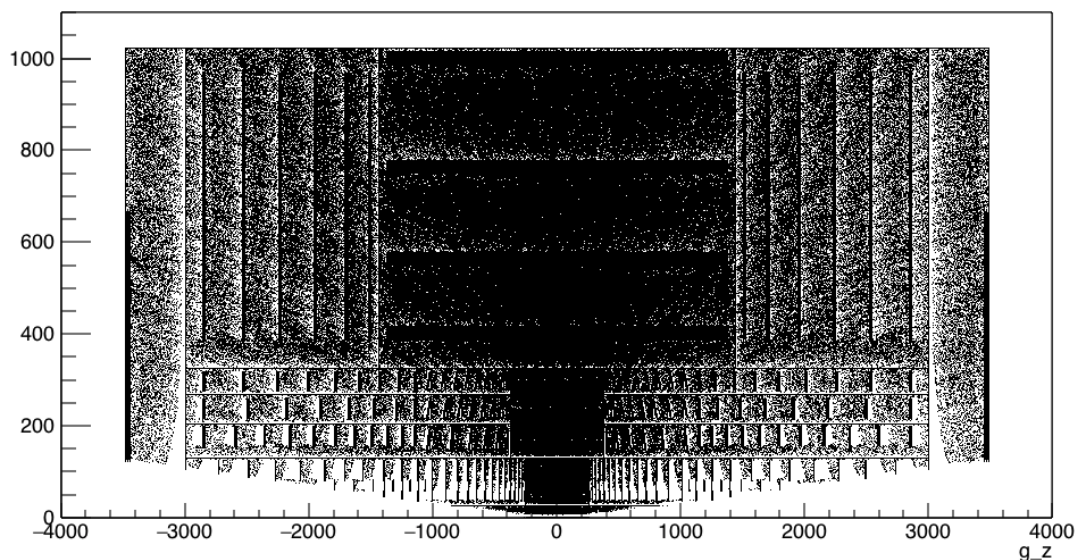


*Figure 2. One million test propagations in 64 threads through the ATLAS ITk detector with the ATLAS magnetic field in ACTS, wall-clock execution time on acts-dev-rd-et of ~1.8 seconds, showing a remarkable performance compared to LHC Run-2 reconstruction. These are identical results to sequential computation, validating the parallel approach.*

Efforts in compute accelerator R&D were aided with the integration of CUDA and SYCL based seeding modules into the continuous integration pipeline of ACTS. This work was extended to support an end-to-end chain of simulation - fast/full simulation - digitization - reconstruction for different input detectors, which will help with future plans to integrate ACTS into Key4hep.

## 2.4 Efficient Analysis

In the EP R&D analysis task, the work in 2020 was connected to efforts to improve ROOT I/O. The broader goal for a next-generation analysis I/O subsystem is to develop and mature HEP data access technology for ultra-fast modern I/O devices. Such devices include 100Gbit/s network cards as well as solid-state disk drives (SSDs) and non-volatile memory (NVM), based on flash memory or phase-change memory (PCM) technology. Such devices are already reaching throughputs of 10GB/s, some 40 times faster than traditional hard disks. For *distributed* analysis workflows, the goal is to develop effective caching mechanisms in order to reuse partial analysis results from repetitive, related analyses. Furthermore, a future analysis I/O subsystem should make optimal use of the distributed object stores that we expect to partially replace distributed file systems in large HPC centers in the next 5-10 years.

Vincenzo Padulano is an R&D funded PhD student, who started in January on distributed caching; and Javier Lopez Gomez, a senior fellow, started in September on connecting the ROOT I/O to the Intel DAOS distributed object store. From the EP R&D material budget, we ordered a test server with a choice of the latest I/O devices available on the market. CERN openlab is kindly providing access to an Intel DAOS distributed object store cluster.

The work on distributed caching evaluated two caching technologies: content-agnostic block-level caching using the XRootD storage system and the application-level caching technology built into ROOT (Figure 3). First results suggest a comparable performance of the two caching technologies. Stability issues in the ROOT caching code were identified and fixed in the process. A CHEP publication on the results is in preparation. Future work aims at improvements in the ROOT caching technology using application knowledge of the data format and the analysis workflow.

The work on distributed object stores resulted in a prototype implementation of an Intel DAOS object store backend for RNTuple, a new experimental ROOT data structure expected to replace TTree. A first performance evaluation shows significantly better performance of the RNTuple native backend compared to the file system compatibility layer provided by DAOS. The RNTuple backend can reach 2GB/s per client read throughput and further improvements are expected to drive the throughput to 5GB/s-10GB/s per client.

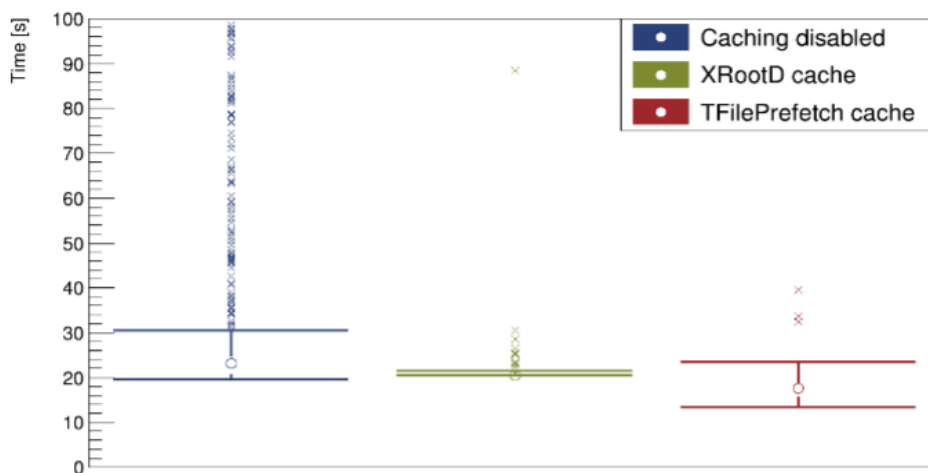


Figure 3. Running times of a synthetic benchmark with a typical analysis I/O pattern reading 1GB of data from remote storage with a 1Gbit/s link. 1000 test runs are executed for each of the three scenarios: uncached, cached by XRootD, and cached by ROOT TFile prefetch. Both caching technologies improve the overall throughput and reduce throughput fluctuations.



### 3. Publications and contributions to conferences and workshops

1. [Key4hep – Plans for deployment](#), Pre-GDB 5 May 2020, Valentin Volkl
2. [CERN R&D on Spack and the Turnkey Stack](#), HSF Workshop 19 November 2020, Valentin Volkl
3. [Tracking aware metric learning for particle reconstruction](#), NeurIPS 2020, Sabrina Amrouche et al.
4. [Storing High-Energy Physics data in DAOS](#), Intel DAOS User Group (DUG), 19 November 2020, Javier Lopez Gomez

## WP8 Detector Magnets R&D

### 1. Introduction

The work package covers the development of a new 4-Tesla general purpose magnet facility, studies in the fields of advanced magnet powering, and innovation in magnet control and safety systems and instrumentation. One fellow has been working from April 2020 on the 4-T magnet studies and on a snubber prototype to suppress the arc in the breakers of the ATLAS Toroidal magnet powering system. One technical student worked from February 2020 until August 2020 on magnet protection, then another student joined from October 2020 to work on magnet design and snubber testing. A second technical student has joined the team in February 2021 to work on cryogenics design.

The 4-T magnet studies focused on two configurations, a split coil and a saddle shape dipole. The conceptual designs have been looked at, and optimization studies are continuing.

The snubber prototype was successfully tested in the TE-CRG Cryolab. This activity will continue with the final design and test of the ATLAS Toroidal magnet snubber system.

As part of R&D infrastructure development, a cryogenic setup is under development. This setup, which will hold a superconducting 5-T solenoid, will be used for sample characterizations.

### 2. Main activities and achievements in 2020

#### 2.1. 4-T magnet facility

The magnetic configurations of the M1 and Morpurgo magnets in the CERN experimental North Area have been considered as starting points for the studies, as a similar inner bore is intended for the new facility, and these magnetic configurations provide the required field transverse to the test beam. The 4-T magnet configurations studied are shown in Figure 1 and Figure 2.

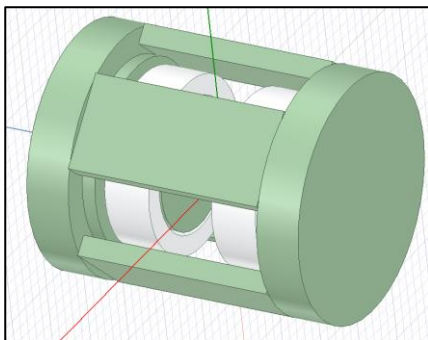


Figure 1. 4 Tesla Split Solenoid Coil

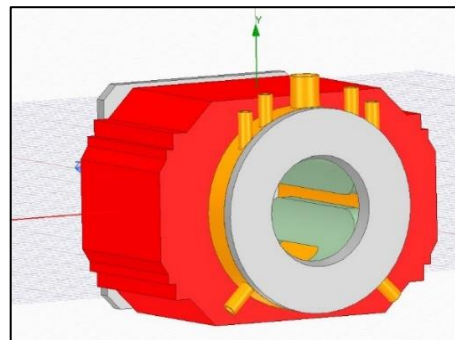


Figure 2. 4 Tesla Saddle Shape Coil

Through various iterations, both the split solenoid and saddle shaped concepts have been optimised to reach the specifications seen in Table 1. Their concepts are based on the designs of the M1 and Morpurgo magnets with similar yoke structures.

The M1-like split solenoid has advantages in its simplicity of manufacture and load support, and a lower peak field in the conductor. The stray field is higher than the existing M1 magnet, therefore a further optimisation of the shielding is on-going. In optimising the winding layout to reduce the peak field, the normally free inner diameter of the solenoid has been filled with iron thereby eliminating the solenoidal direction of use, therefore only providing use as a dipole. An active shielding variant has also been studied but with no benefit due to the limited margin of superconducting properties of the Nb-Ti-based coils.

The Morpurgo-magnet-like saddle shape coil shows promise with regards to stray fields experiencing a maximum of only 5.2 mT at 5 m as seen in Table 11. However, the high peak field on the conductor is less favourable and requires more optimisation on the winding shape.

Table 1. 4-Tesla split solenoid and saddle shape operation specifications.

	Split Solenoid	Saddle Shape
Field at center	4T	
Free warm bore	1.4 m	
Power Supply Current	8 kA	
Total stored energy	95.1 MJ	67 MJ
Peak conductor field	5.18 T	5.9 T
Energy density	11.6 kJ/kg	10.3 kJ/kg
Stray field at 5m	37 mT	5.2 mT

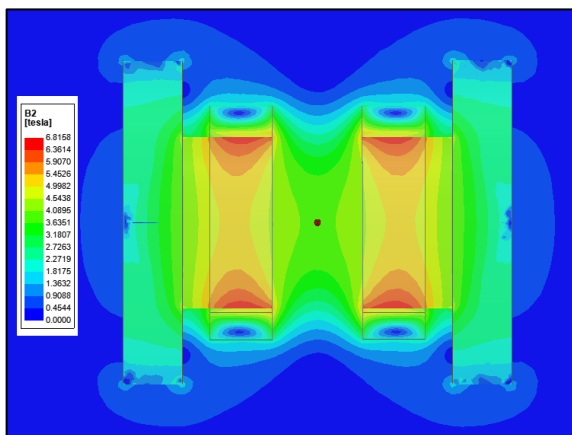


Figure 3. Split Solenoid field map.

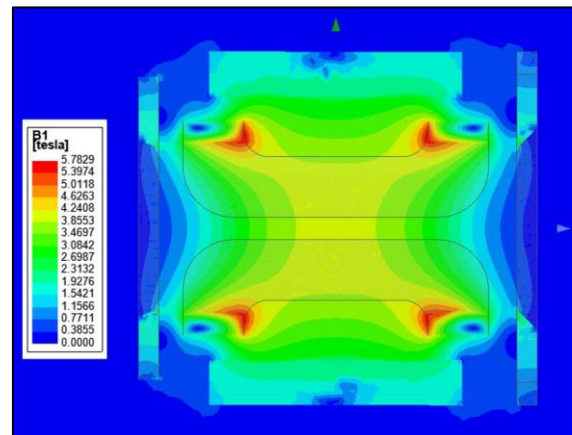


Figure 4. Saddle shape coil field map.

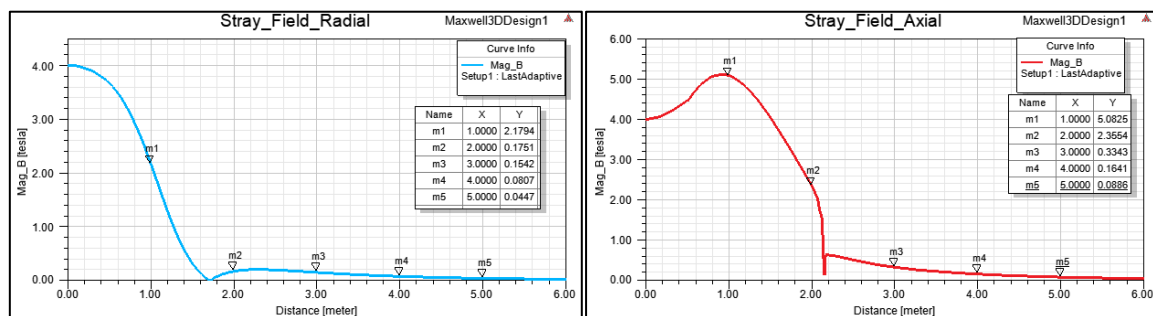


Figure 5. Field values in Radial and Axial directions of split solenoid.

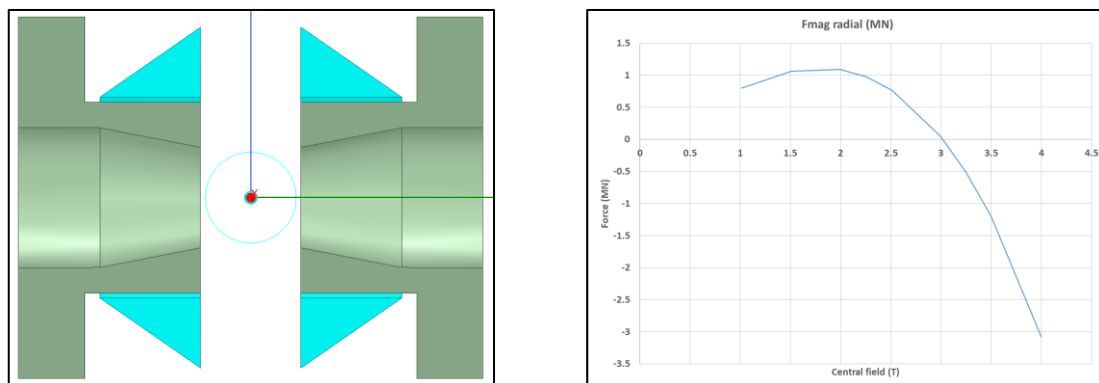


Figure 6. Cone shaped split solenoid concept and inter-coil force of cylindrical shape.

Studies to maintain the dual functionality (solenoidal and dipole) of the split solenoid are ongoing. A promising solution is shown in Figure (left), where the coil and iron shape are optimised to lower the peak field on the superconducting conductor. The direction of the resulting forces applied to the split coils is a function of the central magnetic field (and thus operating current), as seen in Figure (right), requesting a mechanical support to handle the large forces in both directions.

### 2.2. Quench protection studies

To understand the quench behaviour of the preliminary layout of the split coil, quench simulation studies were performed using 'Quench 2.7' [1]. From these studies it was concluded that the coils may be protected through various means. The energy extraction resistors and the quench-back mandrel provide a good safety margin with a peak temperature of about 60 K. With the quench heater variant the coil reaches a temperature of above 100 K, but with a relatively small temperature gradient below 25 K as seen in Figure . This design might be further optimised with the more precise placement and power of the heaters. It shows the feasibility with a reduced temperature gradient across the coil, and the lack of need for energy-extraction systems, resulting in a reduced overall cost for the ancillary systems.

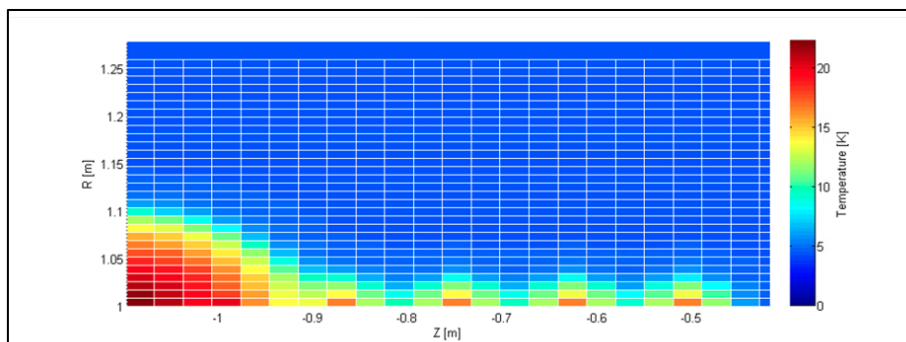


Figure 7. Quench using quench heaters.

### 2.3. ATLAS Toroidal Magnet snubber

The ATLAS Toroidal magnet experiences arcing across its breakers during de-energising. This arcing, resulting from parasitic inductances in the run-down unit, gives increased contact resistance with successive discharges and the risk of over temperature. An arc suppression snubber had been designed and first demonstrated at 1/50<sup>th</sup> scale (Figure 8 and Figure 9). The experimental investigation of the snubber demonstrator showed a successful suppression of arcs, giving confidence in the progression of the overall design effort.

The full-size snubber is to be made up of four individual snubber banks. Currently, additional capacitor endurance tests are on-going, and following successful tests, the setup will be finalised for manufacture, as seen in Figure 10.



Figure 8. Snubber demonstrator tested at Cryolab.

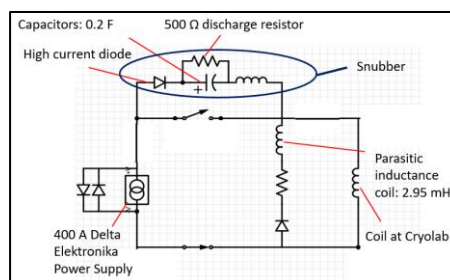


Figure 9. Snubber demonstrator schematic.

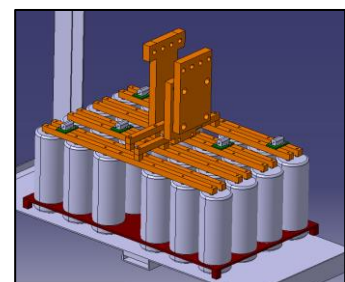


Figure 10. 2.4 F snubber bank.

#### 2.4. Cryogenics

A new test cryogenics facility is under development in order to be able to perform quench and superconductor studies on small prototypes more readily. It shall be installed in 2021. It will benefit from liquid helium Dewar delivery in building 180 provided by the TE-CRG Cryolab. This facility will comprise a custom manifold to interface with a new cryostat equipped with a small 5-T solenoid magnet.

### 3. Summary

Following the start of the EP R&D effort last year, several R&D activities have started in the field of superconducting detector magnets. The efforts are targeted both towards the existing magnets (for example a snubber development for the ATLAS Toroid magnets) and towards future magnet systems such as the Future North Area 4 T User Magnet Facility. These investments, within the context of EP R&D, are helping to support the present and future needs of the CERN organization and the experimental collaborations in terms of superconducting detector magnets.

### 4. References

---

- [1] F. Malinowski et al., “A Quench Analysis for the New North Area Magnet”, EDMS note 2508348 (2020).
- [2] S. Singh et al, “ATLAS Toroidal Snubber Demonstrator”, EDMS note 2466567 (2021).







